The Seybold Report
ISSN 1533-9211
DOI: 10.5281/zenodo.14615527

IMPROVING SOLAR PHOTOVOLTAIC SYSTEMS' PERFORMANCE UNDER PARTIAL SHADING

OSAMA SAAD HAMAD SALEH[1], KALAD SAAD HAMAD SALEH[2] and IZZELDIN IDRIS ABDALLA[3]

[1]Department of Electrical Engineering, Faculty of Technical Engineering, Bright Star University, El Brega City, Libya. E-mail: osamasaadhamad79@yahoo.com
[2]Sirte Company for the Production and Processing of Oil and Gas, Marsa Al Brega, Ajdabiya City, Libya.
[3]Department of Renewable Energy Engineering, College of Energy Technologies, Jikharra City, Libya.

Abstract

The current global energy crisis has driven the need for renewable and sustainable energy sources. Renewable sources of energy, such as hydropower, wind, and solar play a vital part in meeting energy demand. Energy from the sun (solar) remains the most feasible renewable energy source for the generation of electricity in Libya due to its availability throughout the year at excellent irradiation levels. This work is designed to evaluate the impact of partial shade on the Photovoltaic (PV) systems and how to overcome it, as well as propose a correct PV array arrangement for optimal energy generation to supply DC loads. This paper addressed many strategies for "Maximum Power Point Tracking (MPPT) algorithms", such as fuzzy logic control, neural networks, open circuit voltage, perturb and observe, short circuit current, etc. The proposed MPPT algorithm aimed to determine the suitable duty ratio for operating the buck-boost converter to achieve maximum power output. In this work, the MPPT with perturb and observe method is employed, resulting in a significant increase in PV system efficiency. The power and voltage ratings of the PV module employed in this study were 230 watts and 29.9 volts. The PV output voltage can be doubled by using a boost converter. Matlab/Simulink software was also used to simulate the PV system; the simulation results demonstrated that the suggested algorithm can track the global MPP efficiently.

Keywords: Renewable Energy, Performance, Algorithms, Photovoltaic System, Shading.

1. INTRODUCTION

The tremendous increase in energy consumption, particularly in recent decades, has generated concerns about depleting the world's reserves of petroleum and other nonrenewable resources in the near future. The massive usage of fossil fuels has caused apparent damage to the ecosystem in a variety of ways. According to Alrikabi (2014), fossil fuels account for around 90% of our total energy usage. With the increasing global population, the energy demand grows by the day. As a result of the rising energy demand and the need to address conventional energy shortages and environmental concerns, there has been a greater emphasis on cleaner energy sources around the world. Energy from the sun (solar energy) is among the most available renewable energy sources. As a result, solar energy is the potential future of energy in Libya and will be a formidable rival to fossil fuels; this form of energy is harvested using a photovoltaic (PV) system that primarily transforms energy from the sun into usable electrical energy. However, the major problems of this technology remain the high initial project cost, as well as the low conversion efficiency of the PV cells (Aashoor & Robinson, 2012). Solar PV systems for homes, schools, hospitals, government and private organizations buildings, and

ISSN 1533-9211

DOI: 10.5281/zenodo.14615527

industry usually consist of solar panels or panels arranged in strings and strings arranged in big arrays, batteries for power storage, and an inverter. Figure (1) depicts a typical solar PV system in which PV cells attract solar energy and transform it into DC for onward conversion to AC by the inverter. The output power is significantly dependent on both sun irradiance and panel temperature. The intensity of irradiation affects the output power, and high temperatures contribute to considerable power loss (Alqarni and Darwish, 2012; Johari et al., 2011). Many studies have been conducted by researchers aimed at increasing the efficiency of solar PV systems. The MPPT is among the available control techniques for the collection of the most available energy from the PV module (Singh et al., 2015).

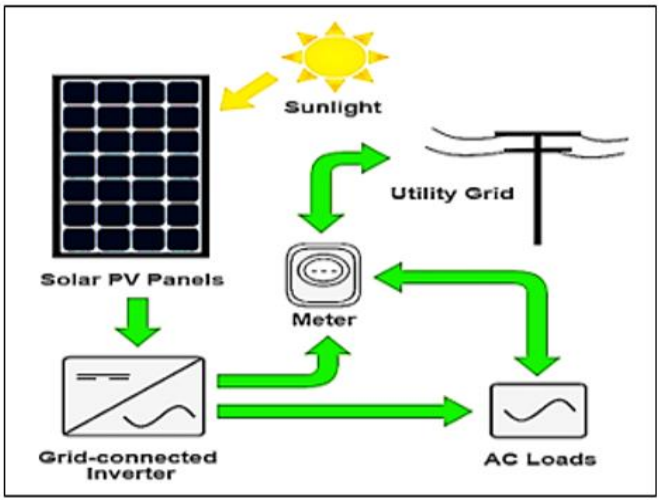

Fig 1: Depiction of a Solar PV System

Source: Behura et al. (2021)

MPPT is a vital component of any solar energy conversion system, but it is mostly implemented at the array level. Figure (2) depicts the placement of MPPT in an ideal solar energy system.

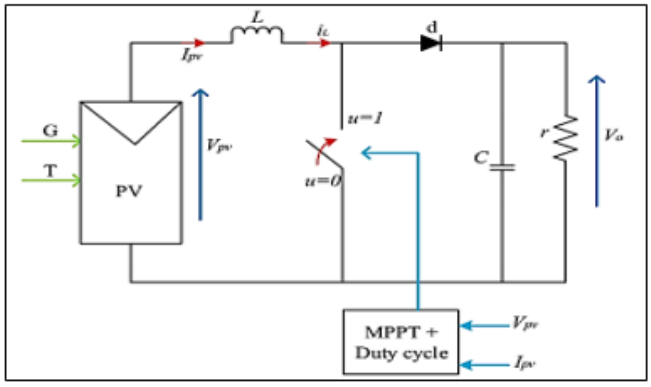

Fig 2: Configuration of MPPT system

Source: Singh et al. (2015)

The Seybold Report
ISSN 1533-9211
DOI: 10.5281/zenodo.14615527

Figure (2) depicts a conventional MPPT system in which irradiance, G, and temperature T function as stimulants for PV outputs. The MPPT algorithm produces the optimal duty cycle for the converter using the PV voltage, PV current, IPV, and VPV as inputs. There have been various MPPT approaches developed and deployed (Singh et al., 2015); each technique differs in intricacy, speed, and accuracy. Each approach has its control variable, such as duty cycle, voltage, or current (Ishaq et al., 2012). The PV system also exhibited steady-state oscillation issues and cannot track the genuine MPP under partial shade conditions (PSC) (Hamidon et al., 2012; Sharma & Purohit, 2012; Elgendy et al., 2012; Ishaque et al., 2014; Ngan et al., 2011; Alajmi et al., 2010). Shading blocks the PV system's current and power flow, and when that happens at night or in complete darkness in general, that can be no problem because batteries would take charge and hence will be no interruption in power flow (Ragb & Bakr, 2023). On the other hand, partial shading is a big problem because it affects the MPP and confuses the system in general; also, the shading has a big effect on solar PV system's energy efficiency (Chiu & Ngo, 2023).

While increasing energy demand has led to shortages and environmental consequences for conventional energy sources, much emphasis has been on renewable sources of energy. Solar energy remains the most available future energy resource that can efficiently replace the current fossil fuels; it is free, available, affordable, and ecologically benign. While traditional fossil fuels have several limitations, including declining reserves and pollution, renewable energy sources, on the other hand, are widely acknowledged to be far cleaner and produce energy without polluting the environment.

Conventional energy generation is one of the biggest contributors to environmental degradation and has a significant impact on human health through greenhouse gas emissions (Hamidon et al., 2012). Renewable energy technologies have gained widespread recognition as critical contributors to the desire for cleaner and sustainable future energy. As a result, an alternate technique of generation must be developed for environmental safety and human health protection. Solar cells or PV cells are small cells that attract and convert energy from the sun into electricity. When PV cells are joined together, they create a module, and connecting many modules contributes to the formation of a solar array (Alajmi et al., 2010).

The PV array is comprised of several modules that are joined together in series or parallel. The array output might vary greatly depending on the amount of irradiation received during the day (Alqarni & Darwish, 2012). Despite the numerous positives of solar energy, it faces significant problems that limit its wide acceptance. The two main issues are low efficiency and a large number of local maxima power.

Using MPPT is an effective strategy for increasing the PV system’s efficiency. The MPPT allows the PV system to function at full power. In reality, conventional common MPPT algorithms may easily determine the MPP in a non-linear P-V curve under constant insolation, but under partial shading, they may fail to track the actual MPP due to various local maxima associated with the P-V curve as illustrated in Figure (3) (Ishaque et al., 2012).

ISSN 1533-9211

DOI: 10.5281/zenodo.14615527

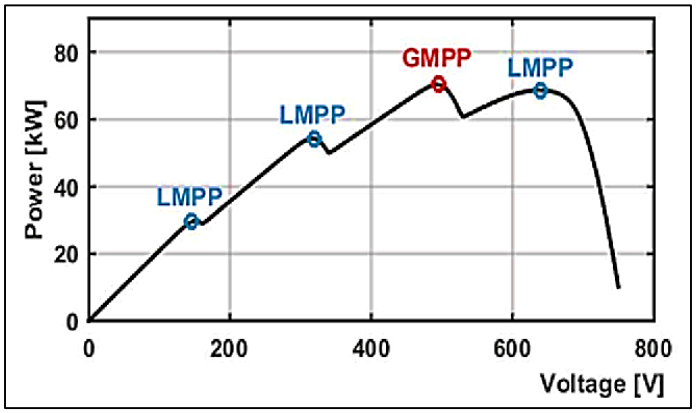

Fig 3: *P-V* curve of PV array under partial shading condition

Source: Avila et al. (2017)

Even though the issue of non-linear output features is a major problem associated with the use of PV arrays, PV sources are gaining application in many areas. If the full array fails to receive consistent insolation, the features become more complicated, as demonstrated in partially shadowed instances. As a result, the existing maximum power point techniques will be less effective since they cannot distinguish between local and global peaks (Ngan et al., 2011). Under PSC, the varying irradiation and temperatures give rise to a PV system with non-linear I-V features, with the P-V characteristic becoming more convoluted with numerous peaks. The partial shading of the PV systems affects the power flow and hence interrupts the work of people in government and private buildings, such as hospitals, schools, and various services. Therefore, it is necessary and motivated to study the problem and find a solution to this problem.

2. PROBLEM STATEMENT

In any evolving energy generation technology, the efficiency of converting light to electricity is low and depends on the technology utilized. For PV technology, the initial project cost is extremely high; however, the technology may be considered thriving these days due to government subsidies. In truth, energy from the sun only reached Earth during the day, with the peak load occurring in the evening. This mandates the use of expensive storage devices such as batteries, which require additional costs for replacement or maintenance over time. Solar energy is strongly reliant on weather parameters and the irradiation changes with location. Hence, there are significant geographical restrictions for solar power generation (Elgendy et al., 2012). The difficulty of being unable to collect the maximum power from partially shaded solar PV is discussed in (Alik et al., 2017). Figure (4) illustrates the PV curve under normal irradiation, whereas Fig. (5) depicts the PV curve under PSC. The PV curve has two peak points: local and global MPP, respectively. The number of bypass diodes employed in the solar determines the number of peak points seen on the PV curve (Pva, 2011).

ISSN 1533-9211

DOI: 10.5281/zenodo.14615527

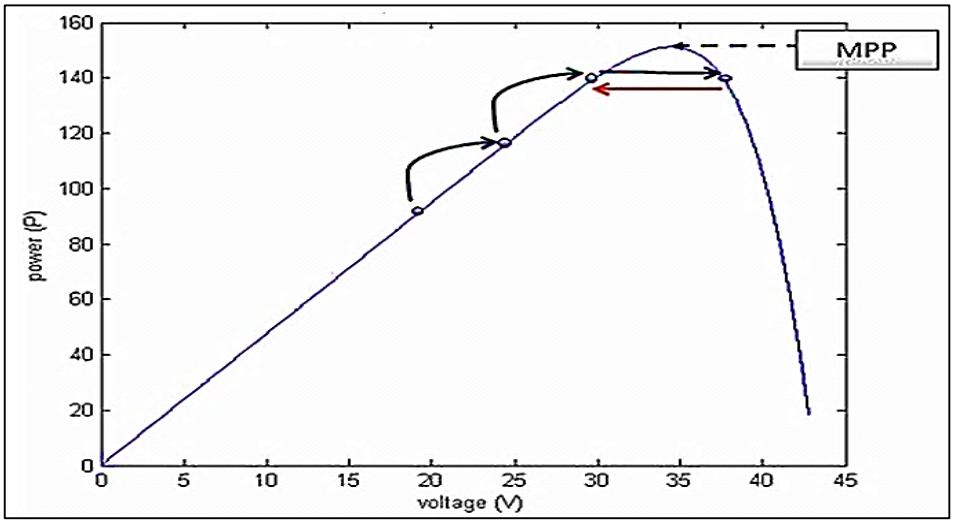

Fig 4: PV curve under normal irradiation

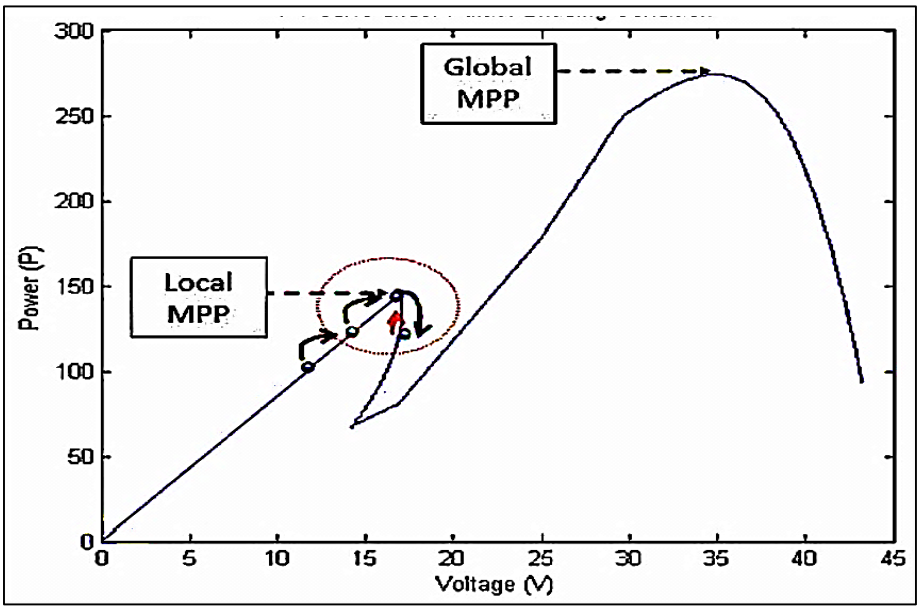

Fig 5: PV curve under PSC

Partially shaded cells on a PV system cannot receive enough radiation from the sun and may get reverse biased by the surrounding high resistance cells. As a result, the temperature would not be uniform across the entire cell area. PSC may also be responsible for the huge power concentration in a small area due to the collapse of a localized region of the cell's p-n junction. Furthermore, PSC can affect PV features such as fill factors, short circuit current, open circuit voltage, etc. (Fialho et al., 2014). These difficulties significantly affect the maximum recoverable power by the MPPT. Considering the ongoing campaign on cleaner energy sources, PV modules are becoming increasingly essential in many sectors, but a major cause of low

The Seybold Report
ISSN 1533-9211
DOI: 10.5281/zenodo.14615527

energy generation in many PV systems is the problem of partial shading. The phenomena of partially shadowed conditions is prevalent in all types of solar systems (Feng, & Ma, 2023). There is a dire need to have full details research to study such a problem and reach some viable solutions. As a result, the tracker should be changed so that it can operate effectively under any irradiation level. Following these, an improved modified tracking system has been proposed in this work.

3. SIMULATION AND RESULTS

The main simulation model of the proposed system in MATLAB/Simulink is presented in Figure (6); it is comprised of serially connected PV modules, a single diode connected in parallel to each PV module, MPPT, a buck-boost converter, a DC load, and scopes for displaying results. Two techniques, namely four serially connected modules and four modules connected in parallel, were implemented and simulated.

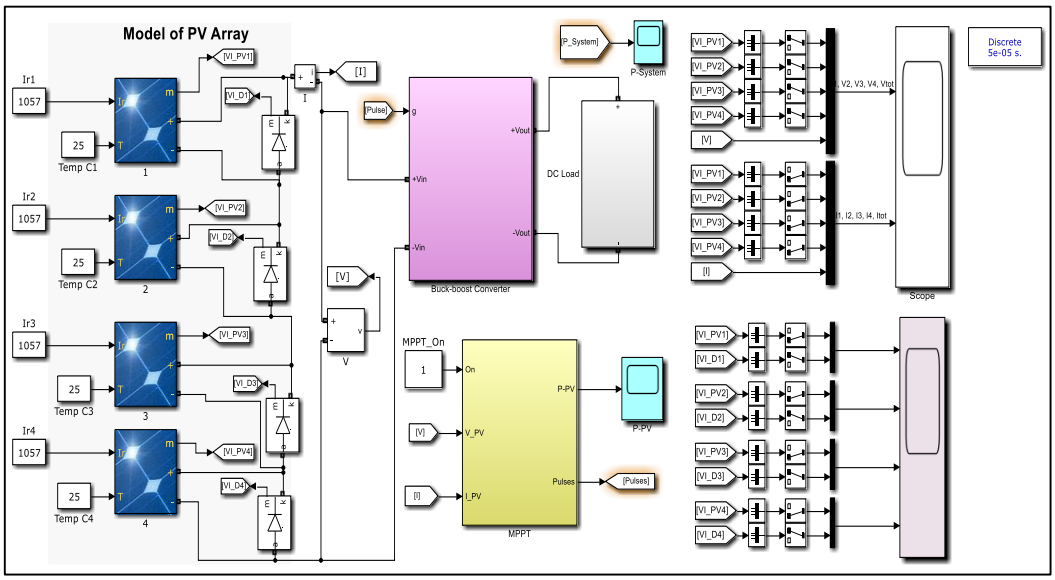

Fig 6: The main simulation model of the system

3.1 PV Module

The PV module is a critical component of the PV system, hence, the PV panel's properties have a considerable impact on energy generation.

3.1.1 Features of PV Module

Figure (7) and Table (1) illustrate the module features employed in this study's simulation where each module consists of 60 cells. The simulation showed that the maximum power was 230 watts while the maximum voltage (VMP) was 29.9 volts, and the maximum current (IMP) was 7.65 amp. The short circuit current (SCC) was 8.18 amps while the open circuit voltage (Voc) was 37.1 volts. The series resistance was 0.34833 ohms, whereas the shunt resistance was 294.1335 ohms.

The Seybold Report
ISSN 1533-9211
DOI: 10.5281/zenodo.14615527

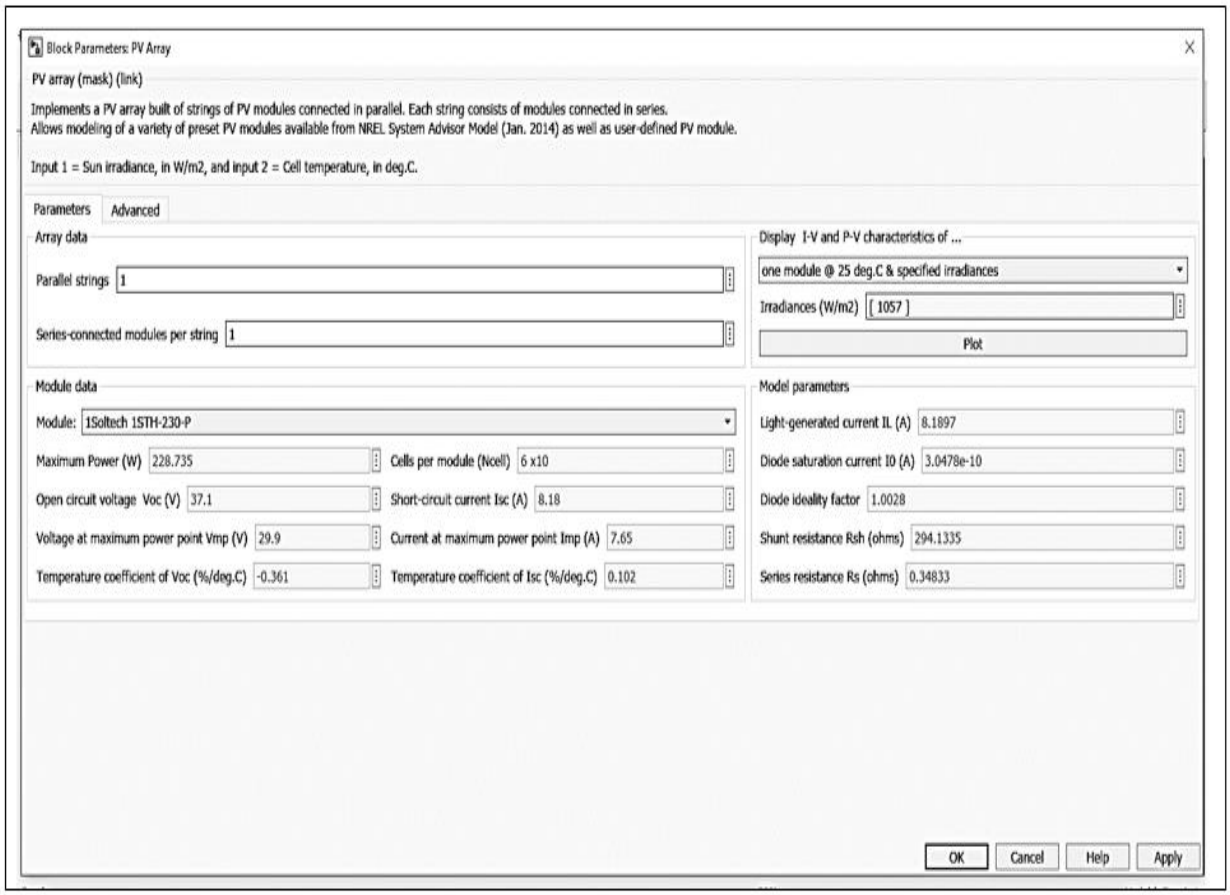

Fig 7: The utilized 1Soltech 1STH-230-P PV module in the simulation

Table 1: Characteristics of PV Module

No.	Parameter	Value
1	Maximum Power	230 W
2	Voltage at maximum Power (V_{MP})	29.9 V
3	Current at maximum power (I_{MP})	7.65 A
4	Open circuit voltage (V_{OC})	37.1 V
5	Short circuit current (I_{SC})	8.18 A
6	Module Efficiency	14.7%
7	Fill Factor	75.8%
8	Power Tolerance	-3.00% ~ 3.00%
9	Temperature Coefficient of I_{sc}	0.102 %/°C
10	Temperature Coefficient of V_{oc}	-0.361 %/°C

Figure (8) depicts the I-V and P-V features of a module; Figure 8 (a) reveals that the current remains constant, but the start lowers when the voltage reaches 29.9 V, whereas Figure 8 (b) reveals that the power increases according to the voltage.

ISSN 1533-9211

DOI: 10.5281/zenodo.14615527

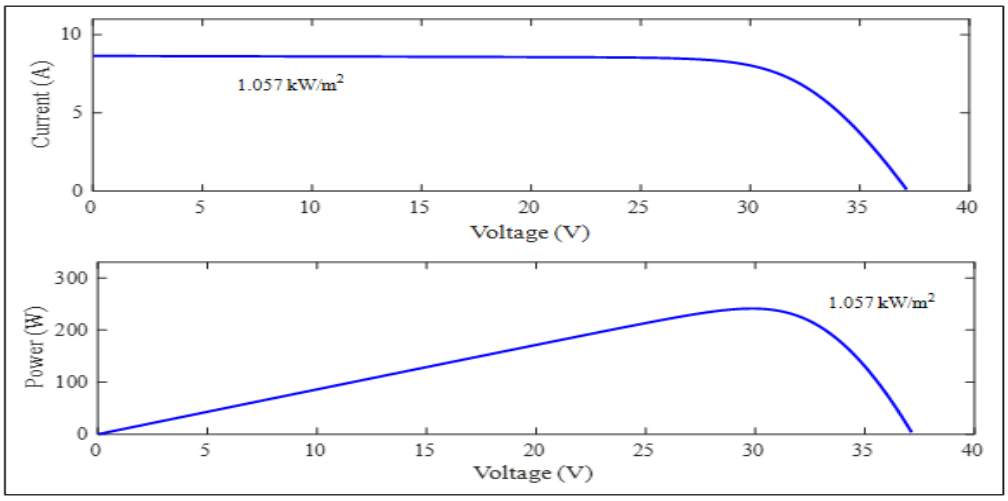

Fig 8: Features of one PV Module; a) I-V characteristic, b) P-V characteristic

Figure (9) depicts the I-V and P-V features of four serially connected modules at T = 25°C and G = 1057 W/m2. The figure shows that connecting the panels in series increased the voltage. As a result, the number of serially connected modules multiplied by the single modules' maximum voltage, which is 29.9 V, yields a total output voltage of 119.6 V from the panels. Furthermore, the power increases according to the voltage and tracks the modules' actual MPP, resulting in a power output of 920 W. However, the current value remained the same at 7.65 A.

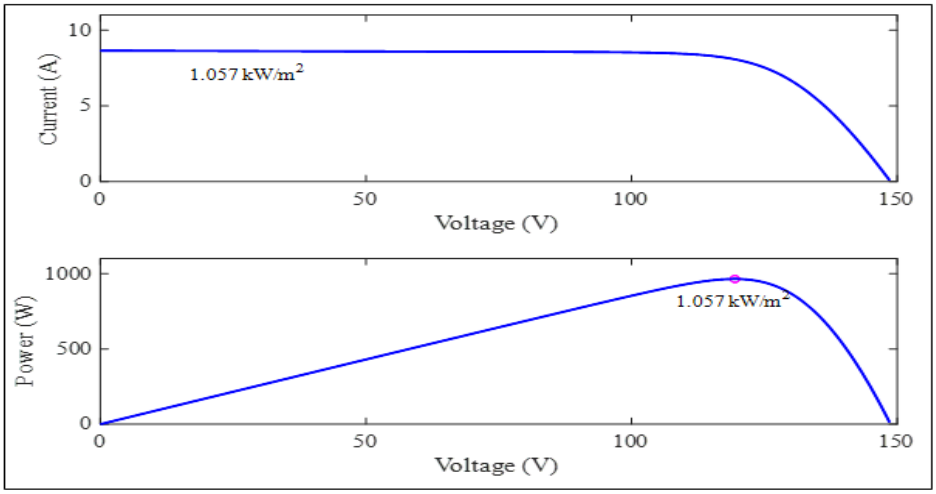

Fig 9: *I-V* and *P-V* features of four serially connected modules at fixed temperature and irradiance

The I-V and P-V features of 4 PV modules linked in parallel at fixed temperature T = 25° and irradiances G = 1057 W/m2 are depicted in Figure (10). Notably, the connection of the modules in parallel did not alter the voltage value as it remained 29.9 V. However, it should be noted that the current increases proportionally with the number of modules.

ISSN 1533-9211

DOI: 10.5281/zenodo.14615527

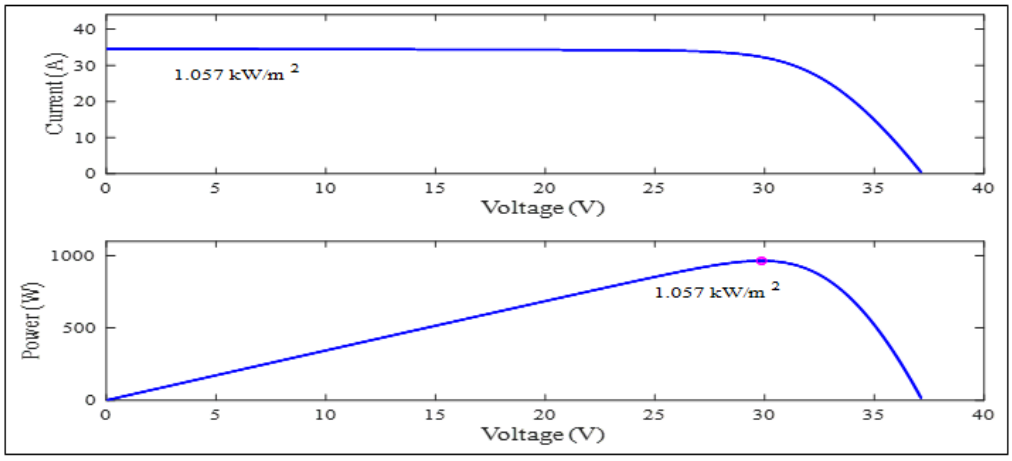

Fig 10: *I-V* and *P-V* features of 4 modules linked in parallel at fixed *T* and *G*

The I-V and P-V features of 4 serially connected modules at fixed *T* and varying *G* (1057, 850, 500, and 200 W/m2) are shown in Figure (11). The chart shows that as *G* varies from 1057 W/m2 to 200 W/m2, the voltage is slightly impacted. Contrarily, the current will decrease correspondingly to the reduction in *G* and as a result, the module's power will decrease as the current decreases.

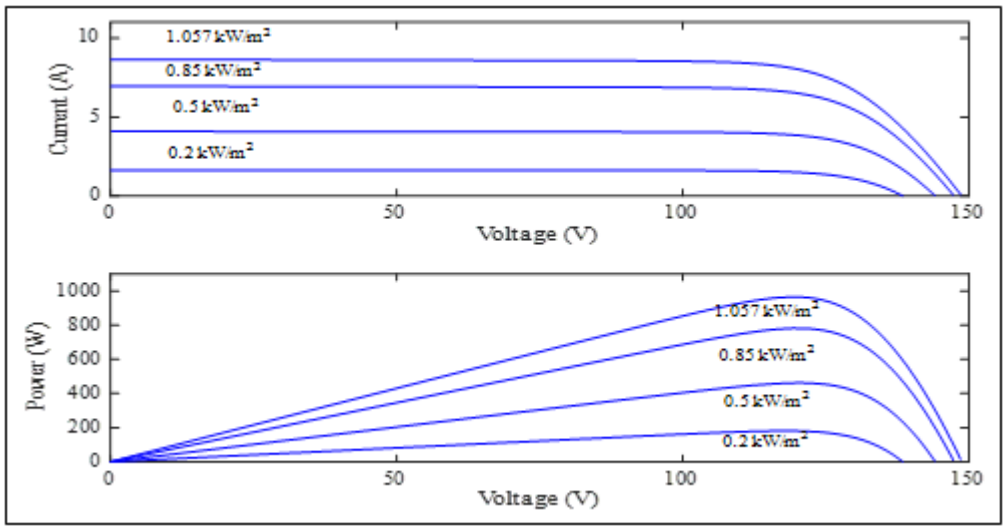

Fig 11: *I-V* and *P-V* features of 4 serially connected modules at fixed *T* and varying *G*

The I-V and P-V features of four serially connected modules at G = 1057 and varying *T* are shown in Figure (12). The simulation results show that at G = 1057 W/m2, the voltage is influenced by the changes in *T*. However, the current was not significantly impacted by the temperature changes and as such, the module's power decreases with drops in the voltage.

ISSN 1533-9211

DOI: 10.5281/zenodo.14615527

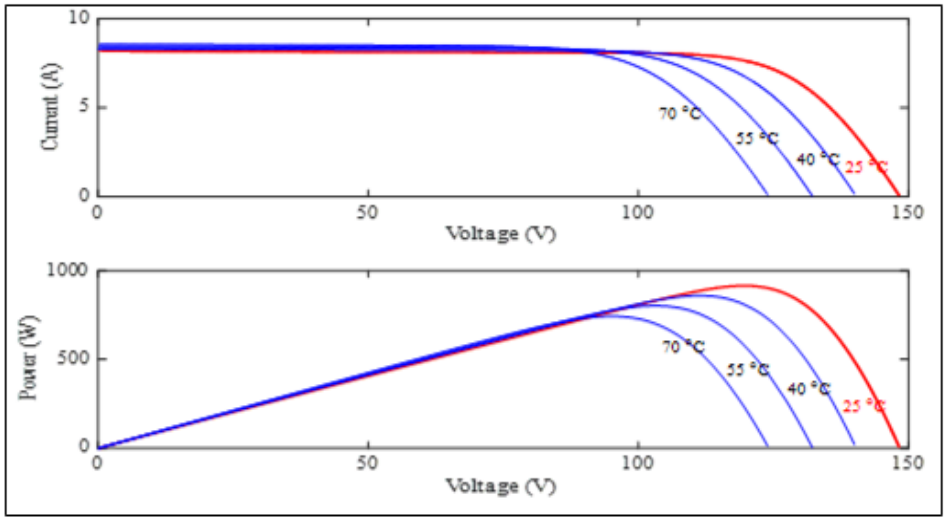

Fig 12: *I-V* and *P-V* features of 4 serially connected modules at fixed *G* and varying *T* values

Figure (13) depicts the I-V and P-V features of 4 modules linked in parallel at T = 25°C and varying irradiances (G = 1057, 850, 500, and 200 W/m^2). The study found that altering irradiances from 1057 W/m2 to 200 W/m2 had a small impact on voltage. Contrarily, the current will decrease correspondingly to the decline in irradiances and as a result, the panel's power will decrease as the current decreases.

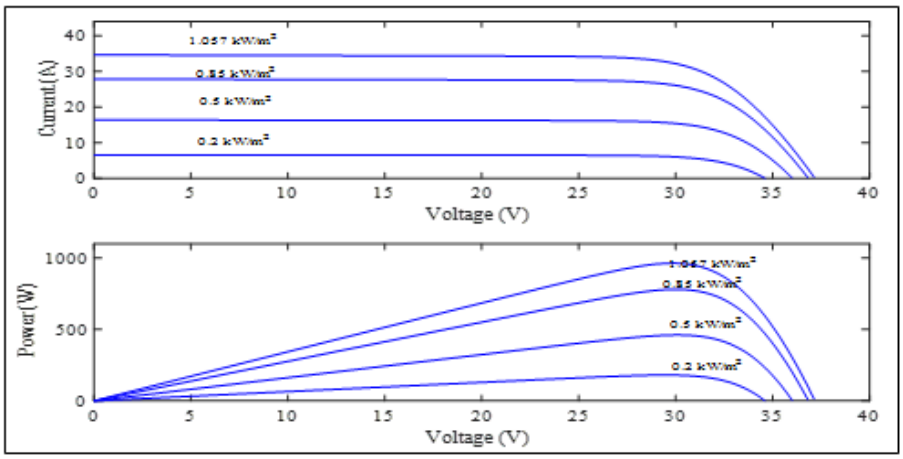

Fig 13: *I-V* and *P-V* features of 4 modules linked in parallel at fixed *T* and varying *G* values

The I-V and P-V features of 4 modules linked in parallel at fixed G and varying T are depicted in Figure (14). Notably, at a constant G value of 1057 W/m2, the changes in T (from 25 - 70°C) affected the voltage but not the current. As a result, the panel's power will decrease due to the decrease in voltage.

ISSN 1533-9211
DOI: 10.5281/zenodo.14615527

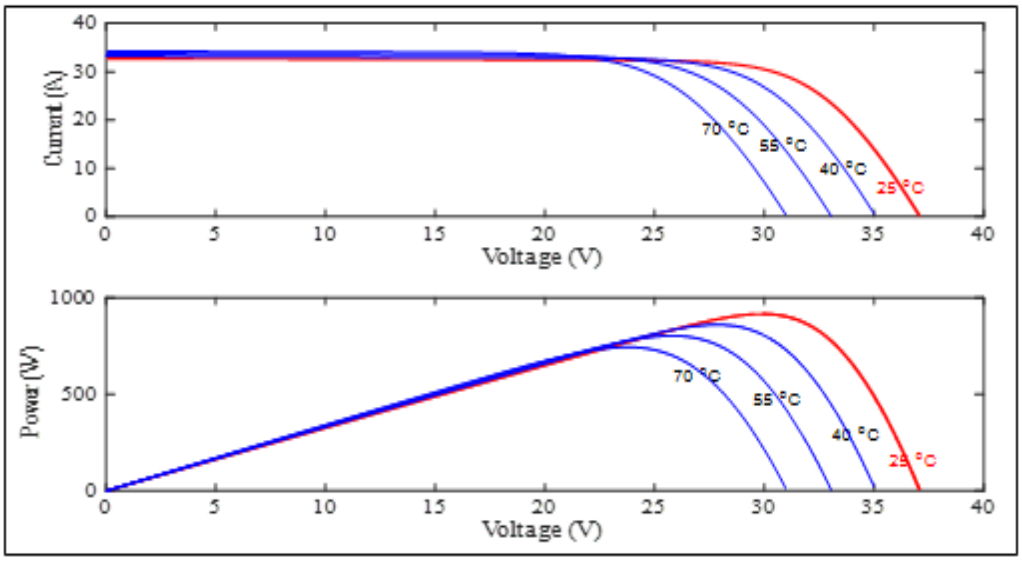

Fig 14: *I-V* and *P-V* features of 4 modules linked in parallel at fixed *G* and varying *T* values

3.2 Maximum Power Point Tracking (MPPT)

Figure (15) depicts a block schematic of the MPPT employed in this investigation; it is comprised of 3 inputs: PV current, voltage, and clock. This MPPT generates the module's power as well as the duty cycle that is fed into the buck-boost converter's gate. Figure (16) depicts a MATLAB/Simulink model of the MPPT with a duty cycle; the graphic shows that the P&O algorithm was employed in the simulation to track the actual MPP.

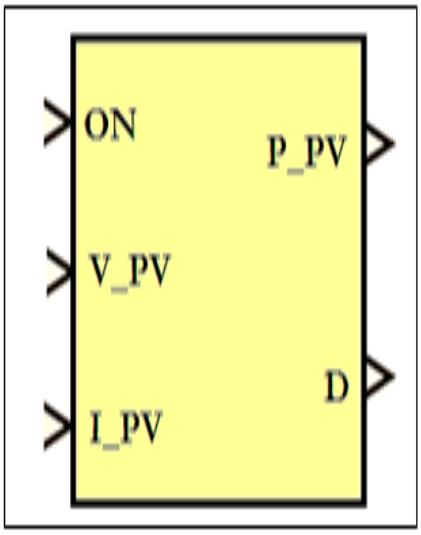

Fig 15: The employed MPPT in this study

ISSN 1533-9211

DOI: 10.5281/zenodo.14615527

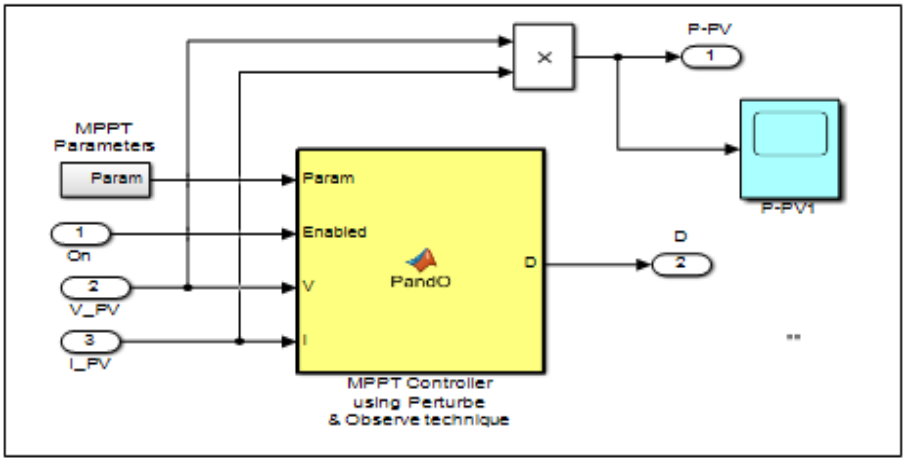

Fig 16: MATLAB/Simulink model of the MPPT using the P&O algorithm

The code for an MPPT controller employing the P&O algorithm is listed below. This code contains all the commands that are important in tracking the actual MPP and regulating the system's output power oscillation. Furthermore, it can distinguish between the old and new powers. It also offers the option to alter the additional ratio of the duty cycle that is fed into the converter.

```
function D  = PandO(T, Enabled, V, I)
 % MPPT controller based on the Perturb & Observe algorithm.
 % D output = Reference for DC link voltage
%
% Enabled input = 1 to enable the MPPT controller
% V input = PV array terminal voltage (V)
% I input = PV array current (A)

persistent P2 P1 dP d  dd n;
 dataType = 'double';
 if isempty(V)
    Vold=29;
  End
if isempty(I)
I= 0;
  End
if isempty(P2)
   P2= 0;
```

The Seybold Report
ISSN 1533-9211
DOI: 10.5281/zenodo.14615527

```
 End
if isempty(P1)
  P1= 0;
  End
if isempty(dP)
dP= 0;
  End
if isempty(d)
d= 1;
  End
if isempty(dd)
dd= 0;
  End
if isempty(n)
n= 1;
  End
%%%%%%%%%%%%%%%%%%%%%%%%%%%%%%%%%%%%%%%%%%%%%%%%%%%%%%%%
 if (T > n*0.02) % chu ki lay mau 0.0;
   n = n+1;
      P1=P2;
      P2=V*I;
        dP= P2 – P1;
   if (dd==0)            D = Dold - deltaD;
   if dP > 1
      dd=0.009;
      d = d + dd;
  else
     if dP < -1     ;
      dd=-0.009;
      d = d + dd;
  else
          dd=0;
End
   End
```

The Seybold Report
ISSN 1533-9211
DOI: 10.5281/zenodo.14615527

```
else
  if ((dP<1 && (dP>-1))
   dd=0;
   d = d + dd;
else
   if ((dP/dd)>0)
     dd=0.009;
     d = d + dd;
else
 dd= -0.009;
 d = d + dd;
End
  End
    End
      End
D=d/(d+1);
if D<0.1
   D = 0.1;
d=D/(1-D);
else
if D>0.9
D = 0.9
d=D/(1-D);
else
  End
    End
      End
```

Figure (17) depicts a MATLAB/Simulink model of the DC converter that can regulate the output voltage. The circuit design's primary components and features are the capacitor, control signal, filter, inductor, switching frequency (FS), and IGBT switch. In this circuit, the utilized switching frequency $Fs = 300\ KHz$. The circuit was designed using a capacitor $C = 200$ µF and inductor $L = 329$ µH.

ISSN 1533-9211

DOI: 10.5281/zenodo.14615527

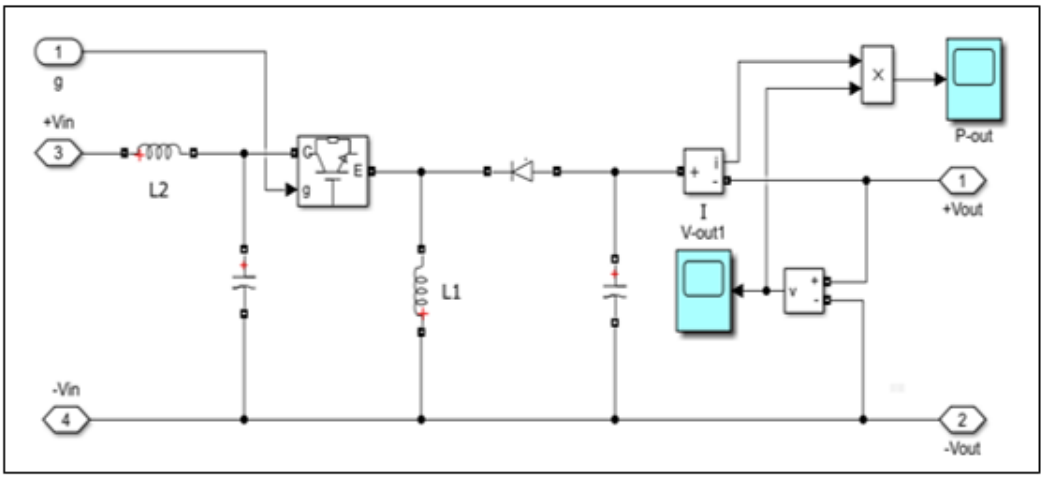

Fig 17: MATLAB/Simulink model of the Buck-boost converter

3.3 Four Serially-Connected Modules at Constant Temperature

The simulated model of the 4 serially connected modules at fixed G = 1057 W/m2 and T = 25°C, together with a single diode connected to each module in parallel is shown in Figure (18).

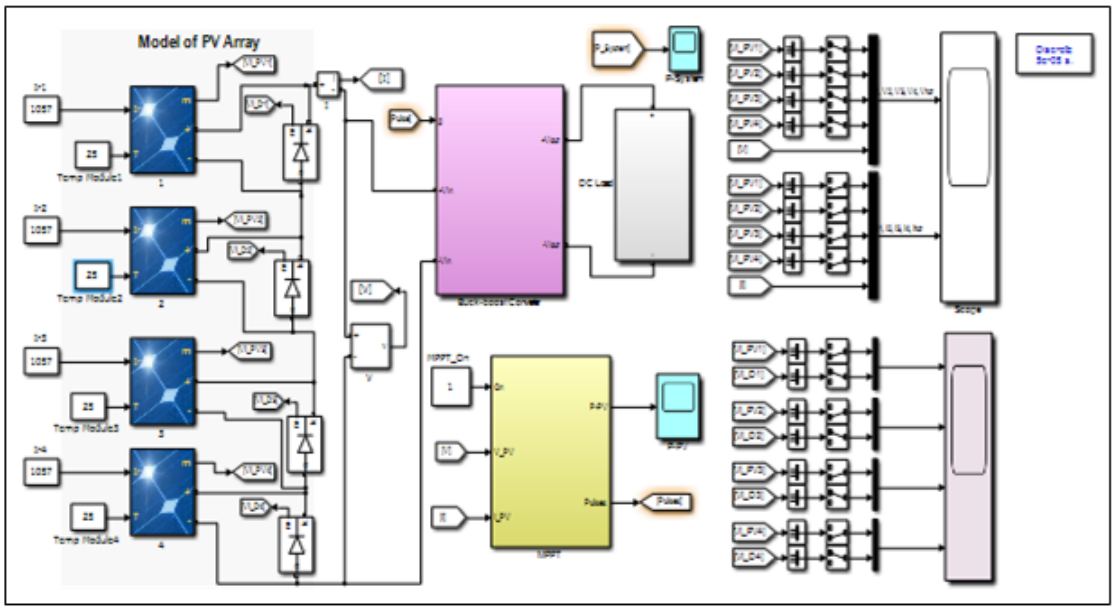

Fig 18: Four serially connected modules with constant G and T, at a duty ratio of 0.05

The system and module's output power using the depicted simulation model in Figure (13) at a duty ratio of 0.05 is shown in Figure (19). The four modules exhibited an MPP of 920 watts, the output power of 919.94 W, and system's output of 918.2 W. The system's output power losses can be attributed to switching losses associated with the PWM switching circuit, as well

ISSN 1533-9211

DOI: 10.5281/zenodo.14615527

as the losses in the converter circuit. Hence, the use of theP&O–based MPPT boosted the PV system's efficiency to around 99.81% with slightly high oscillation due to the change of about 0.05 in the duty ratio.

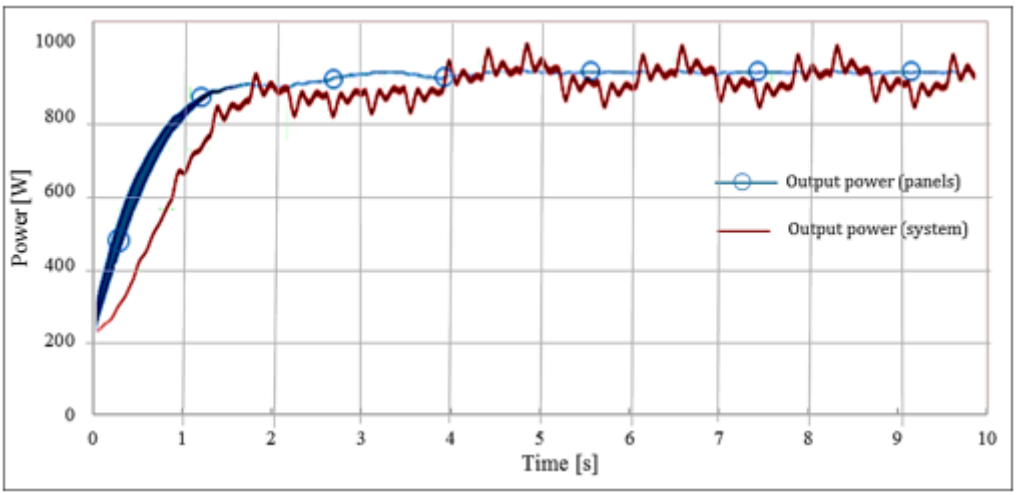

Fig 19: The output power of the modules and the system with a duty ratio of 0.05

Figure (20) displays the output power waveforms of the modules and system, based on the presented simulation model in Figure (13) at a duty ratio of 0.009. Observably, the panel and system's output power reached a steady state quickly as compared to Figure (21). This graph also showed reduced oscillations due to the drop of about 0.009 in the duty ratio; however, the system's efficiency remains quite high.

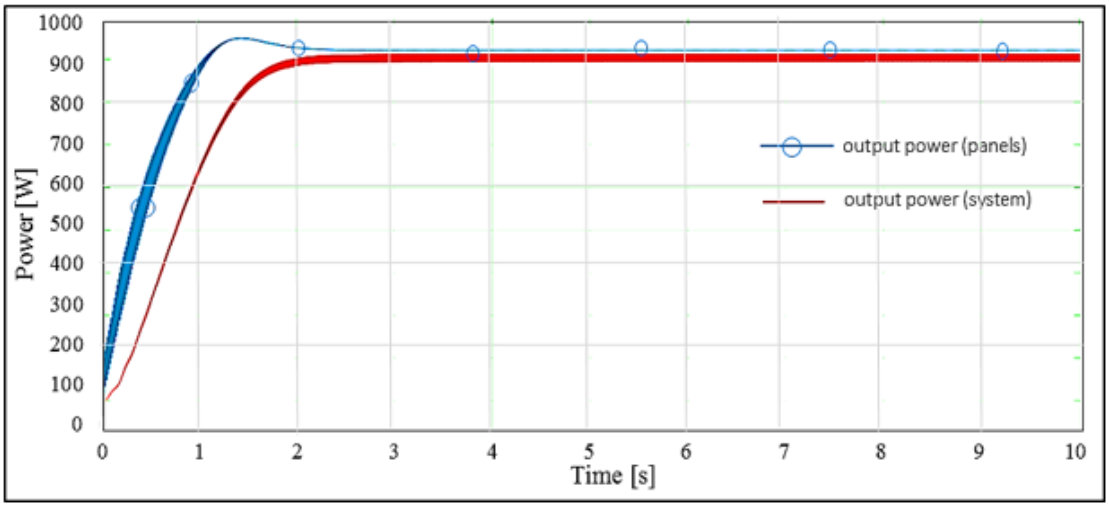

Fig 20: The module and system's output power at a duty ratio of 0.009

The model of the four serially connected modules (one panel irradiated at 700 W/m^2 and three others at 1057 W/m^2) at fixed *T* and a duty ratio of 0.05 is depicted in Figure (21).

The Seybold Report
ISSN 1533-9211
DOI: 10.5281/zenodo.14615527

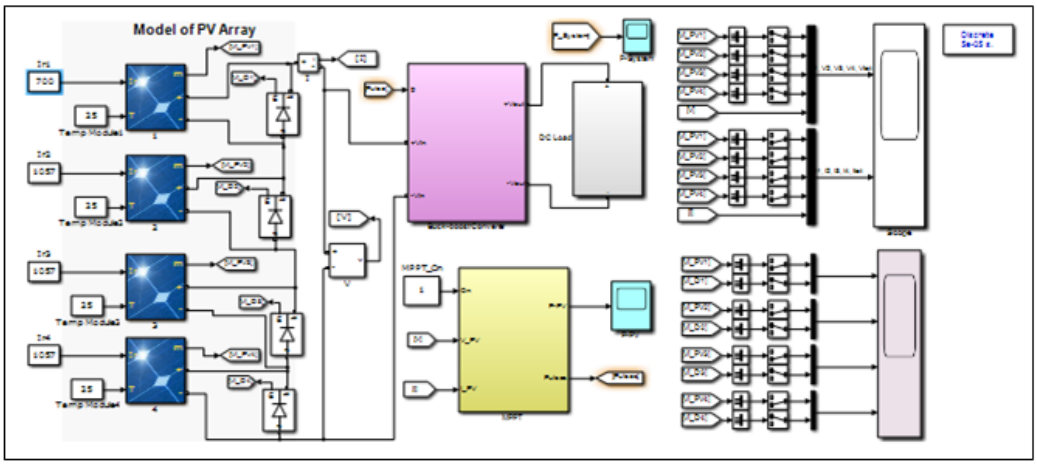

Fig 21: Four serially connected modules at constant T (one module is irradiated at 700 W/m^2) and a duty ratio of 0.05

Figure (22) displays the modules and system's output power waveforms based on the presented simulation model in Figure (16). As seen in Figures (16 and 17), when the shadow hits the first module at G = 700 W/m2, there were changes in the panel and system outputs, with a predicted module output of 888.655 W after partial shading and actual output modules of 737.2 W, and system's output of 724.1 W. The efficiency is good, at 98.2%, and high oscillation was seen due to a duty ratio of 0.05 applied to the new duty cycle; the duty cycle, D = 0.5652.

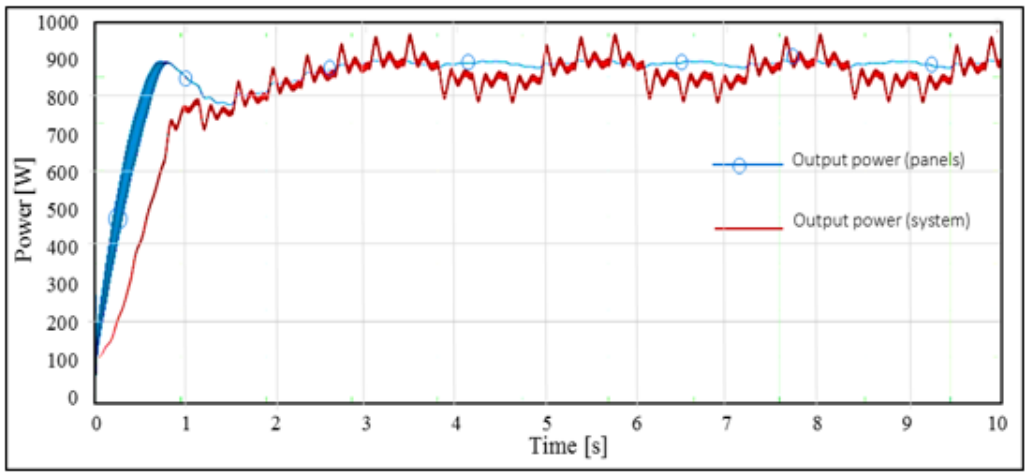

Fig 22: The modules and system's output power at a duty ratio of 0.05 at fixed T and one module irradiated with 700 W/m^2

Figure (23) depicts a simulation model of 4 serially connected modules with one panel exposed to *G* = 700 W/m2 and the other three exposed to *G* = 1057 W/m2 at a fixed *T* and duty ratio of 0.009.

The Seybold Report
ISSN 1533-9211
DOI: 10.5281/zenodo.14615527

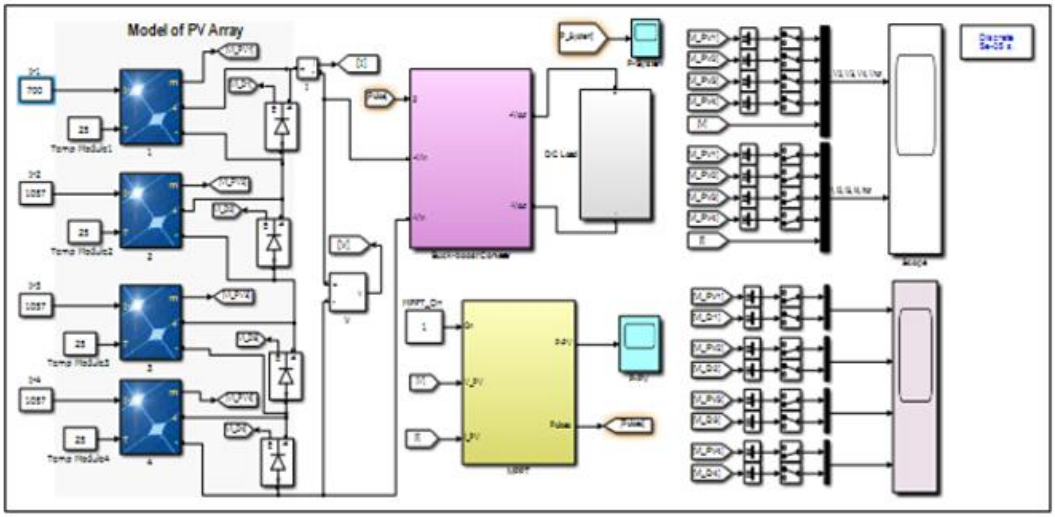

Fig 23: Four serially connected modules with a fixed *T* and one module irradiated with 700 W/m^2 and duty ratio of 0.009

Figure (24) depicts the modules and system's output power from the simulation model in Figure (18). According to Figure (19), when the shadow hits the first module with G = 800 W/m2, there were alterations in the modules and system output. The anticipated module output after partial shading is 888.655 W. However, the output modules produced 768.2 W, whereas the system's output was 761.6 W. The efficiency remained good at 99.14% and the oscillation improved than earlier due to the alteration of the duty ratio (0.009); the output results rapidly reached steady-state.

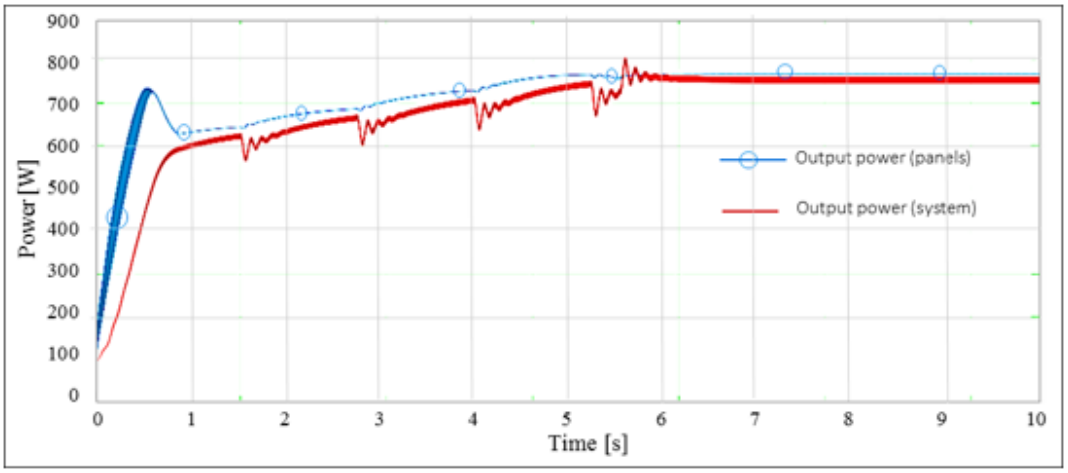

Fig 24: The module and system's output power at a duty ratio of 0.009 and constant *T*; one module is irradiated differently from others

In Figure (25), the four serially connected modules are presented, with one module being exposed to G = 800 W/m^2 and the other three with G = 1057 W/m^2 at fixed T.

The Seybold Report
ISSN 1533-9211
DOI: 10.5281/zenodo.14615527

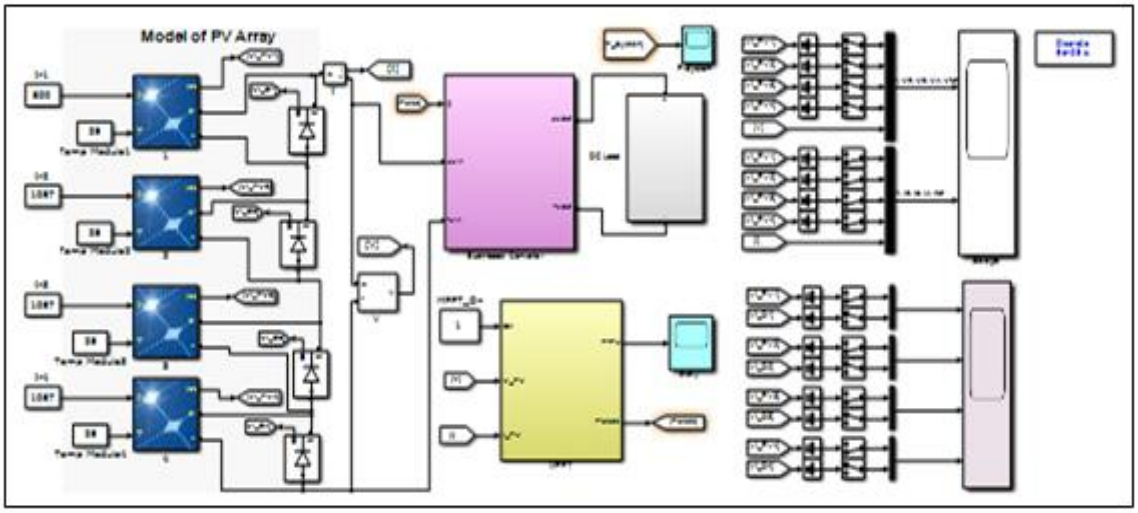

Fig 25: Four serially connected modules with one module irradiated with 800 W/m^2 and the other three with 1057 W/m^2 at fixed *T*

Figures (26 & 27) illustrate that when a shadow of G = 800 W/m2 reaches the first module, it affects both the module and system output. The optimal modules' output after the shadow effect must be 909.97 W; however, the output panels generate 828.7 W, while the system produces 820.7 W. The efficiency remained good at 99.03% and the oscillation is severe due to the added duty ratio (0.05) to the new duty cycle; the obtained duty cycle, D = 0.4872.

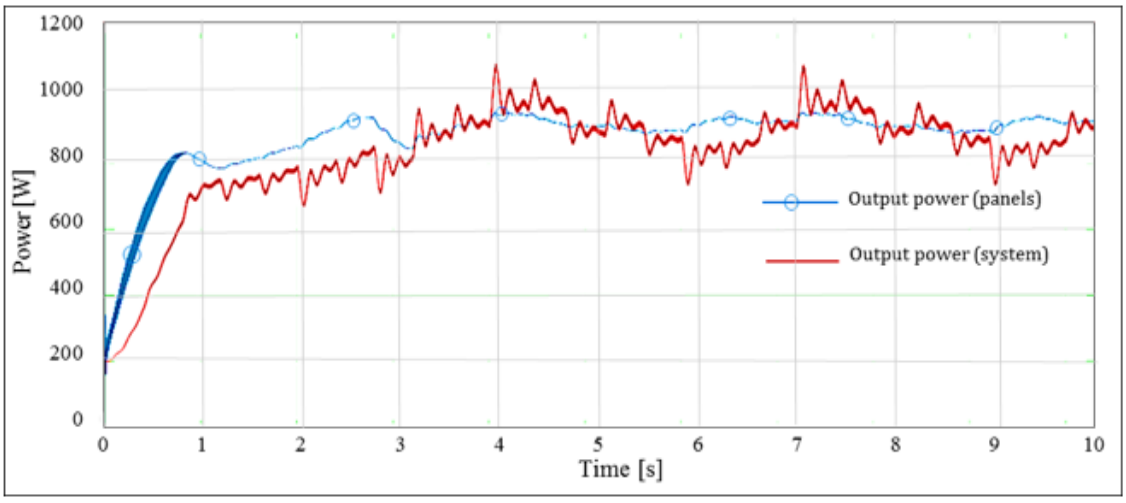

Fig 26: Output power of four series modules and the system with duty ratio 0.05 at fixed *T* and one module differently irradiated

Figure (27) depicts 4 serially connected modules, with one module exposed to G = 800 W/m2 and the other three exposed to G = 1057 W/m2 at fixed T and duty ratio of 0.009.

The Seybold Report
ISSN 1533-9211
DOI: 10.5281/zenodo.14615527

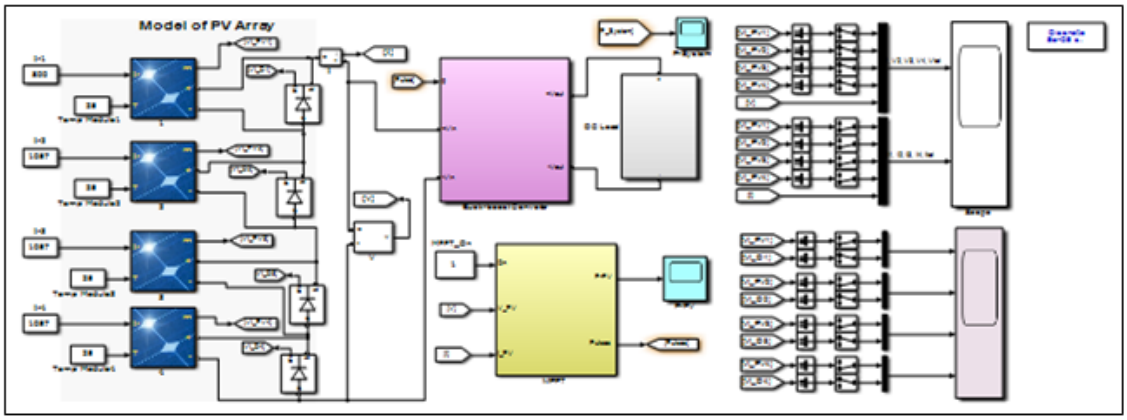

Fig 27: Four serially connected modules with one module irradiated with 800 W/m^2 at fixed *T* and duty ratio of 0.009

When the first module is partially shaded by G = 800 W/m2, the system and module's output are influenced (Figures 28 & 29). The estimated output of the panels after the influence of shadow must be 909.97 W; the output power modules produce 848.1 W, whereas the system's output is 826.3 W. The efficiency is exceptionally good, at 97.43% and the duty ratio (0.009) added to the new duty cycle, completely reduces the oscillation; duty cycle, D = 0.4932.

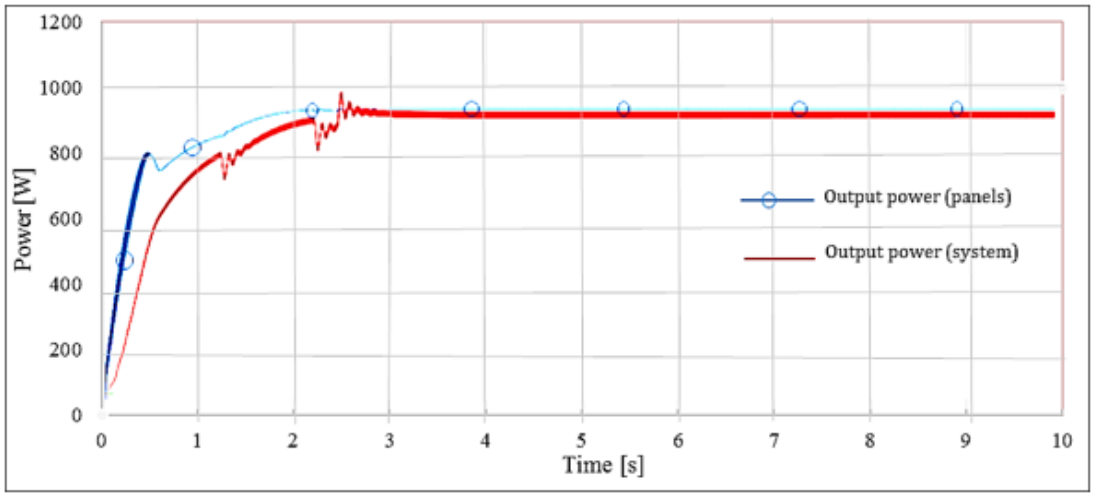

Fig 28: Modules and system's output power at fixed *T* and with one module irradiated with 800 W/m^2 with a duty ratio of 0.009

Figures (29 & 30) show that a partial shade of 900 W/m2 on the first module and 1000 W/m2 on the other three panels affects module and system output power. The optimal output of the modules after the shadow effect must be 901.285 W; however, the output modules produce 881.7 W, whereas the system's output is 873.2 W. The efficiency is great (99.04%) and the oscillation is minimized by the added 0.009 to the duty ratio; the circuit's duty cycle, D = 0.5131.

The Seybold Report
ISSN 1533-9211
DOI: 10.5281/zenodo.14615527

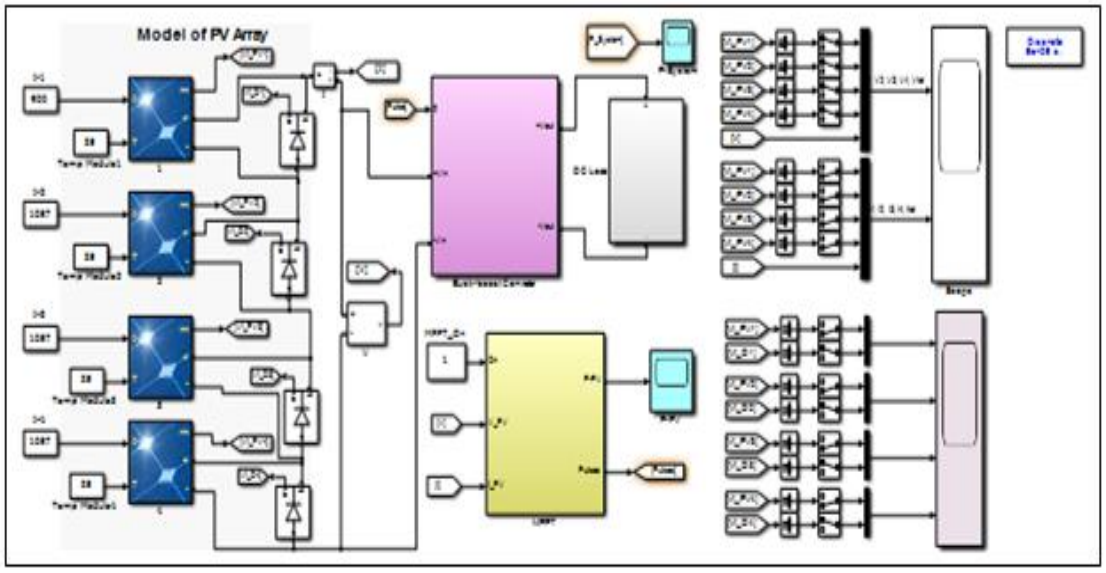

Fig 29: Four serially connected modules at fixed *T* with a duty ratio of 0.009 and one module irradiated with 900 W/m^2

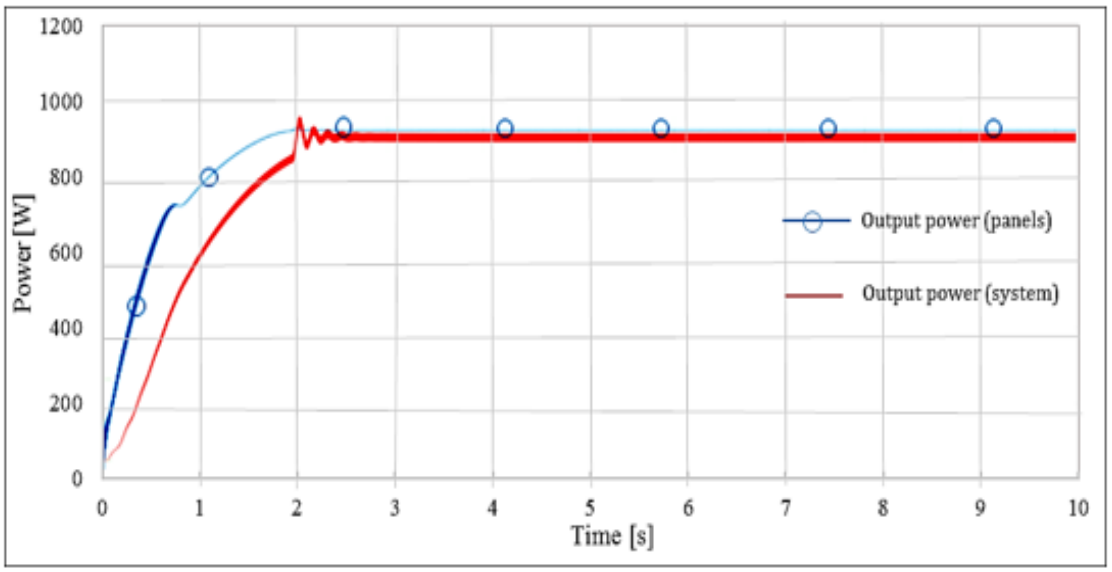

Fig 30: Modules and system's output power at fixed *T* and duty ratio of 0.009; one module is irradiated with 900 W/m^2

3.4 Four Serially-Connected Modules with Constant Irradiance

According to Figures (31 and 32), the output of the panels is seriously affected when the irradiance is constant (1057 W/m2) and one module is fixed at $T = 10°C$; drops in T increase voltage and vice versa.

ISSN 1533-9211

DOI: 10.5281/zenodo.14615527

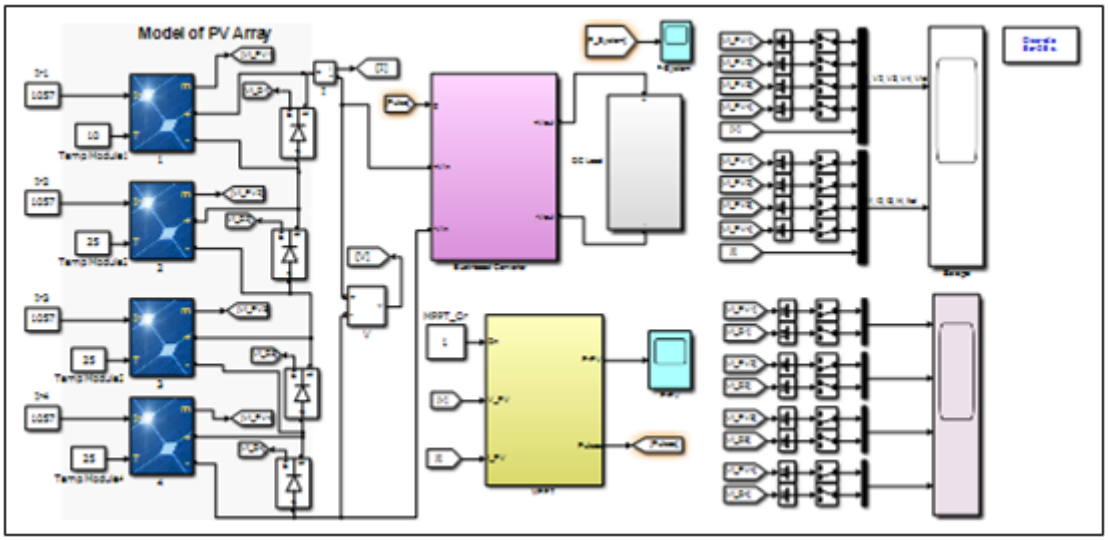

Fig 31: Simulink model of four serially connected modules at constant G and one module at $T = 10^{o}C$

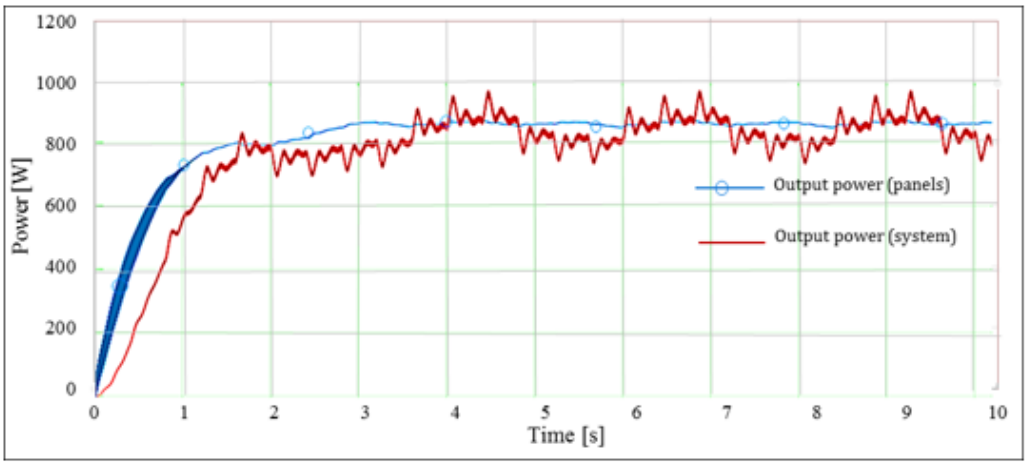

Fig 32: Module and systems' output power at fixed G and one module at $T = 10^{o}C$ and duty ratio = 0.05

The temperature-affected module reached an output voltage of 7.936 A, and the current of the module was 7.936 A. After the temperature effect, the expected modules' output is 920 W, but the actual value is 930.3 W, while the systems' output is 891.6 W, giving an efficiency rate of 95.8%; high oscillation is noted due to the added 0.05 to the duty ratio; duty cycle, D = 0.5122.

ISSN 1533-9211

DOI: 10.5281/zenodo.14615527

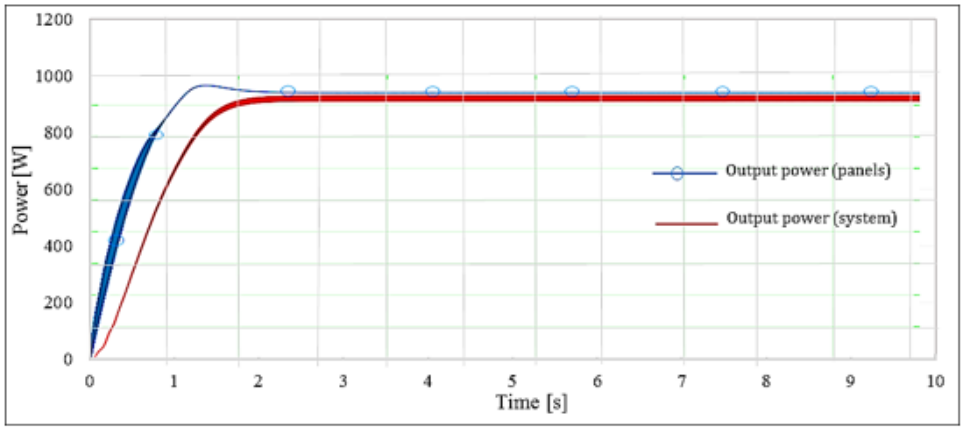

Fig 33: Modules and system's output power at fixed G and one module at T = 10°C and duty ratio = 0.009

Figure (33) demonstrates that the oscillation is degraded as a result of the added duty ratio (which equals 0.009) to the new duty cycle, and the output of the four modules and the system reaches a steady state rapidly. The obtained duty cycle, D = 0.5074. The temperature-affected module's current is 7.562 A, its output voltage is 33.38 V, and the combined output voltage of the 4 modules = 123.08 V. A situation where G is fixed at 1057 W/m2 and T is varied at T = 50°C is depicted in Fig.s 34 and 35. The module and system's output are influenced inversely. Temperature increases reduce the voltage falls, and vice versa. The data reveal a decrease in the output voltage as the temperature increases. Hence, there are drops in the modules and systems' output. The modules' output power = 863.4 W, whereas the system output = 842.8 W. The efficiency is approximately 97.6%; the temperature-affected module has a current of 7.54 A and an output voltage of 28.5 V.

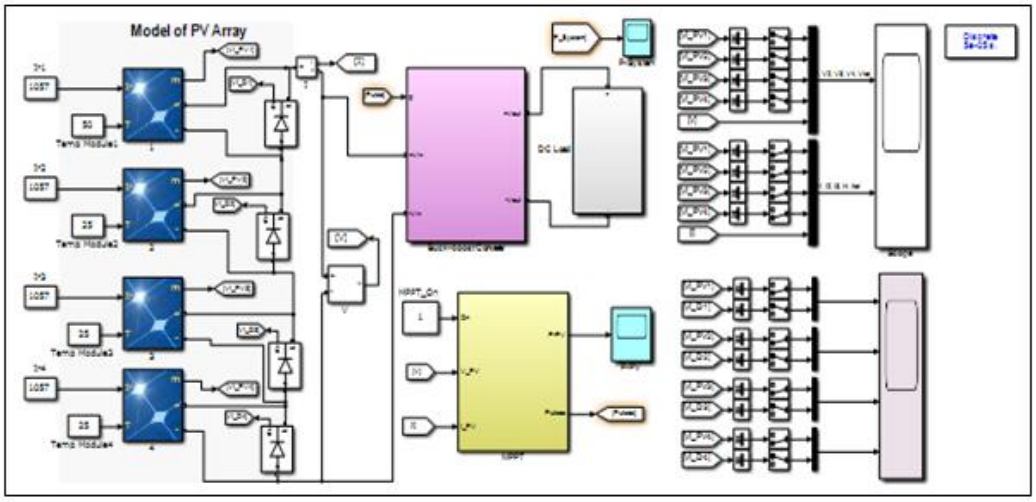

Fig 34: Simulink model of four serially connected modules at constant G and the first module at T = 50°C

ISSN 1533-9211

DOI: 10.5281/zenodo.14615527

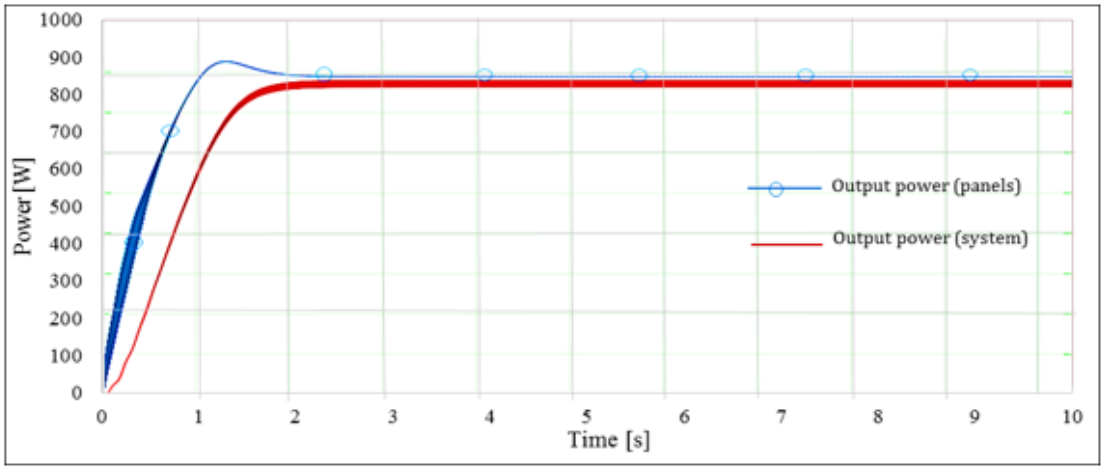

Fig 35: Output power of four serially connected modules at fixed G and the first module at T = 50°C

3.5 Two Serially-Connected Modules and Two Connected in Parallel with Fixed *T*

Figs. 36 and 37 show the Simulink model and output power of four modules, two are linked parallel and two are in series; one module is exposed to G = 800 W/m2 and the other to G = 1057 W/m2.

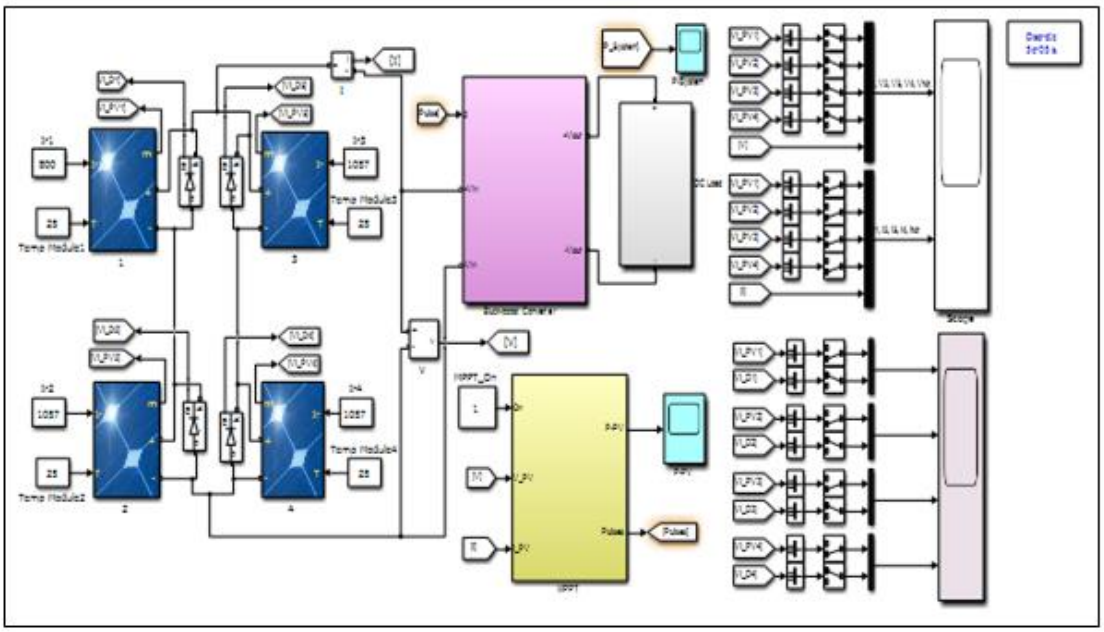

Fig 36: Simulink model of four modules - two are serially connected and two in parallel; one module is exposed to G = 800 W/m^2 and the other to G = 1057 W/m^2

The Seybold Report
ISSN 1533-9211
DOI: 10.5281/zenodo.14615527

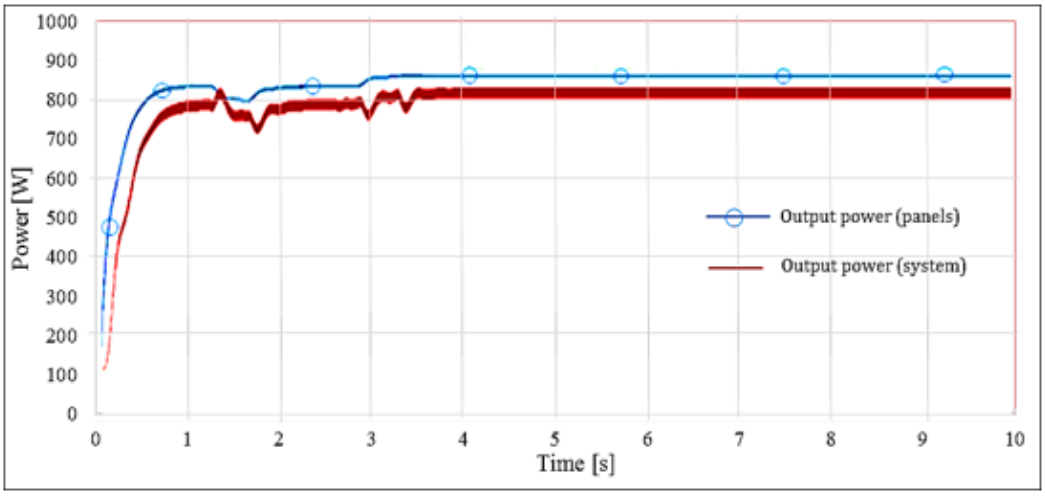

Fig 37: Output power of the system with four modules - two are linked in parallel and two are in series; one module is exposed to G = 800 W/m^2, duty ratio = 0.05

The perfect output power would be 879.97 W at G = 800 W/m2. The modules output = 887.8 W, while the system outputs 823.2 W. The two serially connected modules produce a current of 7.024 A due to the shadow, while the two modules linked in parallel output 7.31 amps. The duty cycle equals 0.4845 and the added ratio equals 0.02. The system's resistance load is 6 ohms and the efficiency is 92.7%. The ΔD is 0.009 and the duty cycle is 0.5067. Figure (33) demonstrates that reducing the duty cycle ratio almost eliminates oscillation.

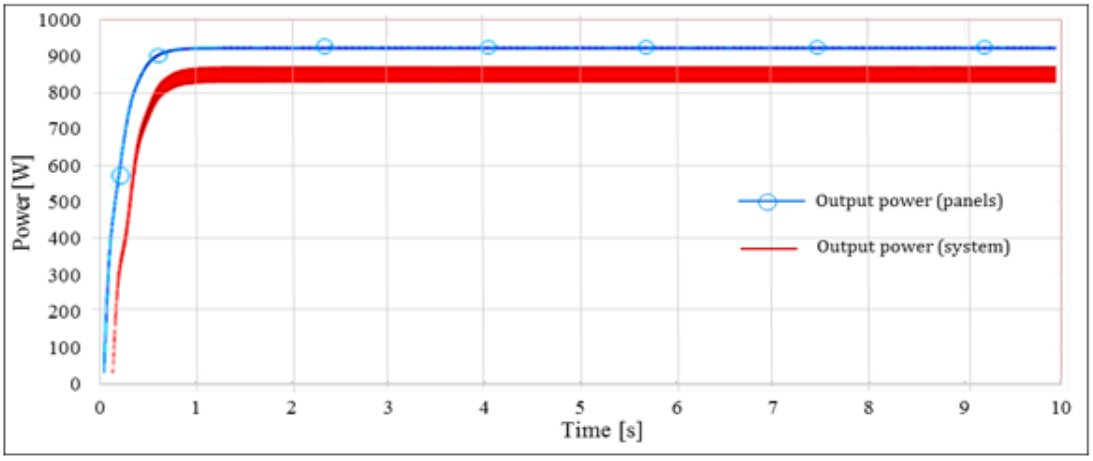

Fig 33: Output power of the system with four modules - two modules are serially connected while the other two are connected in parallel; duty ratio = 0.009; one module irradiated at 800 W/m^2

Figures (34, 35, and 36) show the Simulink model and output power of 4 modules (2 modules are serially connected and the other two are connected in series); for one of the modules, G = 700 W/m2 and for the other three modules, G = 1057 W/m2; temperature is fixed. It is expected

The Seybold Report
ISSN 1533-9211
DOI: 10.5281/zenodo.14615527

that the ideal output power would be 888.655 W; however, the actual modules' output was 843.8 W, whereas the total output is 795.8 W. The two serially connected modules had a current value of 6.107 A, which has decreased due to the shadow effect. For the two modules linked in parallel, the current reading is 7.589 A. The value of the duty cycle = 0.4845 and the added ratio = 0.02. The resistance load = 5 ohms, and the efficiency reached 94.3 %; a significantly high oscillation is noted (see Fig. 35).

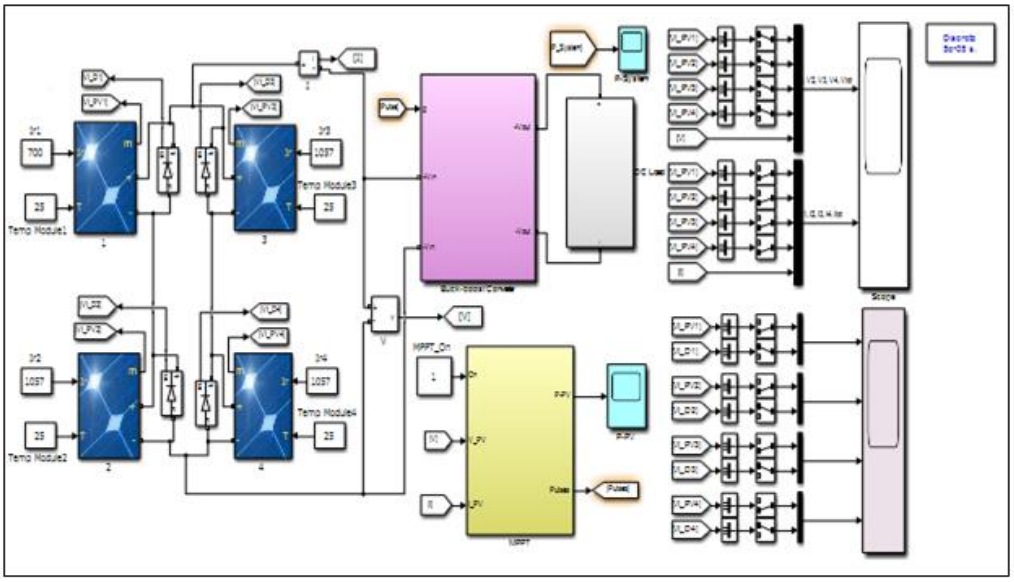

Fig 34: Simulink model of four modules where two modules are serially connected and two are linked in parallel at fixed *T* and *G* = 700 W/m² in one module

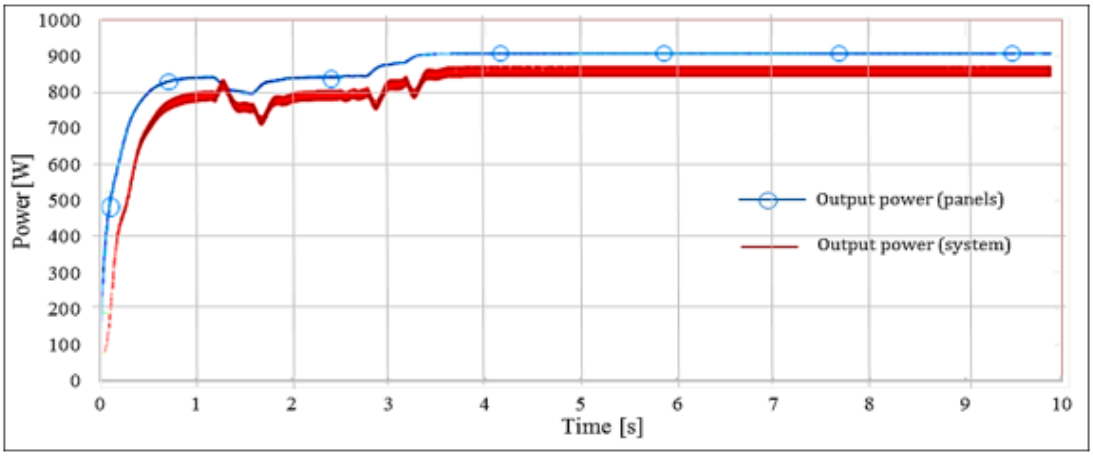

Fig 35: Output power of the system where two modules are serially connected and two are linked in parallel at fixed *T* and with *G* = 700 W/m² in one module

The value of the duty cycle = 0.5067, and ΔD = 0.009; the reduction in duty cycle almost eliminated oscillation as seen in Fig. 36.

ISSN 1533-9211

DOI: 10.5281/zenodo.14615527

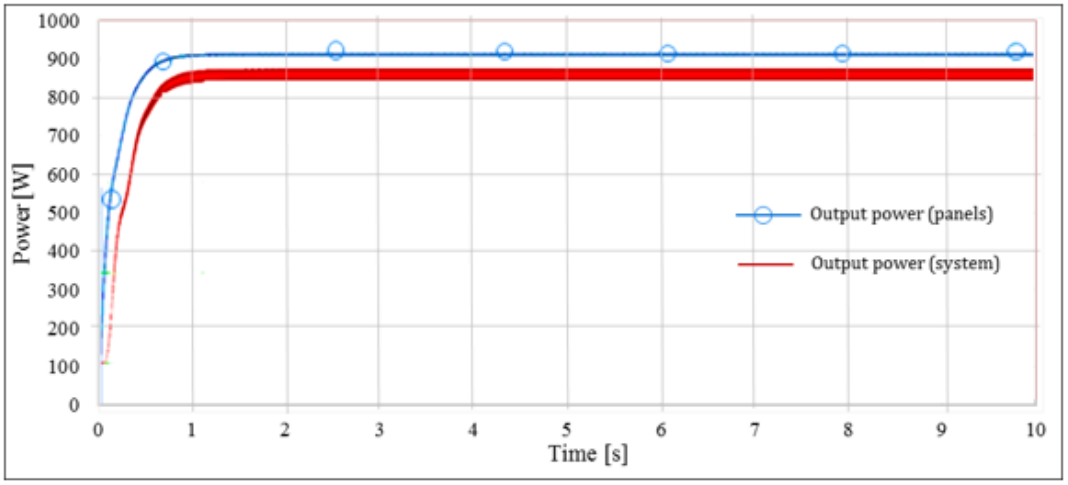

Fig 36: Systems' output power with two serially connected modules and another two modules connected in parallel at fixed T and $\Delta D = 0.009$ with $G = 700$ W/m^2 in one module

The output power and Simulink model of 4 modules in which two are serially connected and two are linked in parallel at $T = 25$°C and $G = 1057$ W/m2 in all modules is shown in Figures (37 and 38). The projected output power is 920 watts but the actual output power = 919.8 W; the system's output power = 861.1 watts. The current produced by the four modules = 7.65 A at a duty cycle value of 0.5098 and an added ratio of 0.02. Efficiency = 93% and the resistance load = 5 ohms.

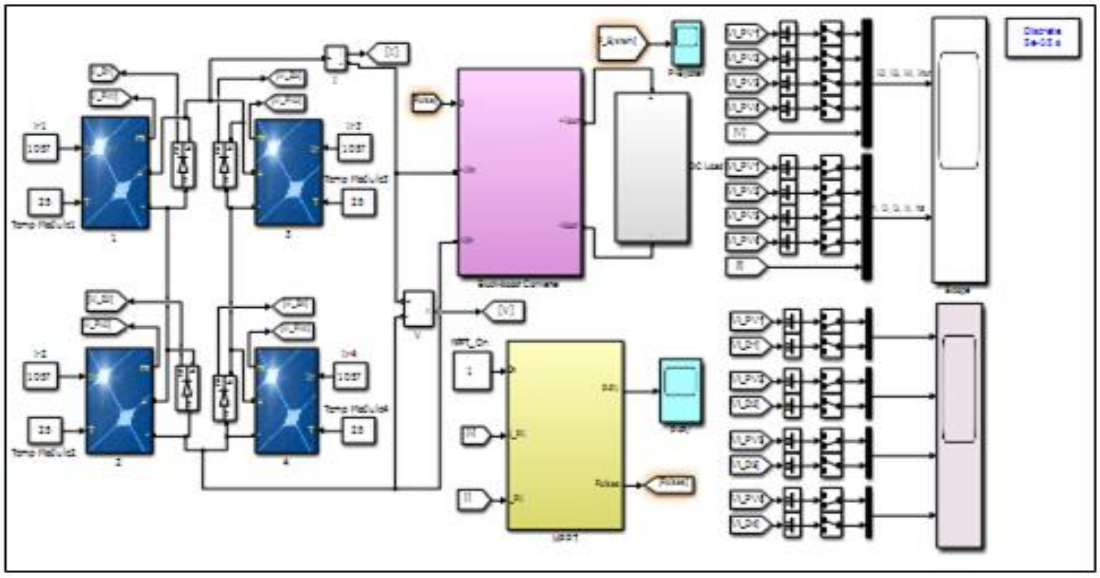

Fig 37: Simulink model of four modules where two are serially connected and two are linked in parallel, at $T = 25$°C and $G = 1057$ W/m^2

The Seybold Report
ISSN 1533-9211
DOI: 10.5281/zenodo.14615527

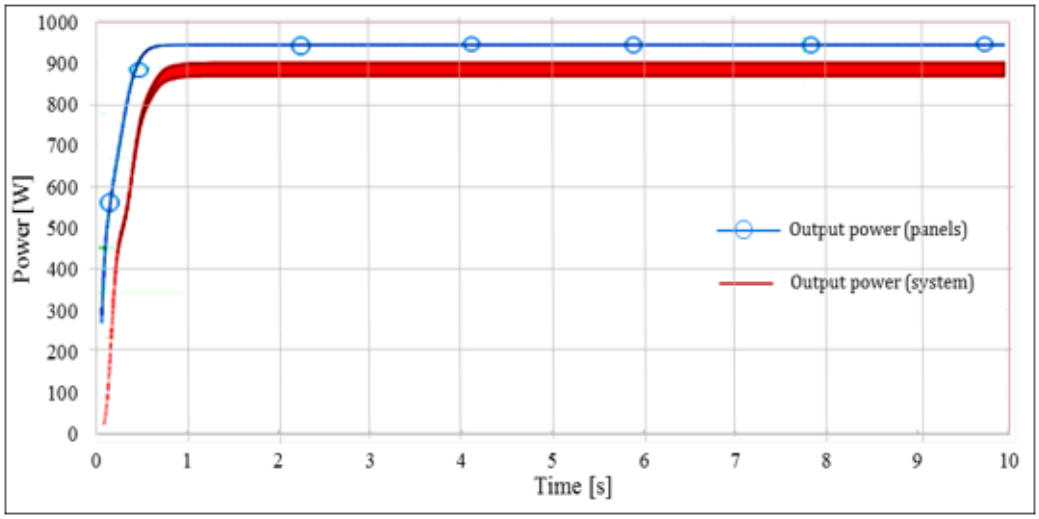

Fig 38: Systems' output power where two modules are serially connected and two are linked in parallel, at $T = 25^{o}C$ and $G = 1057$ W/m^2

3.6 Two Serially-Connected Modules and Two in Parallel with Fixed *G*

Fig.s (39 & 40) depict the Simulink model and output power of a system where both the temperature and shadow are fixed; the system and the panel output are set to the panel's maximum power. The panels' projected output power is 920 watts and after simulation, the output panels generate 919.2 W, whereas the system produces 869.8 W. The efficiency is 94.6 percent.

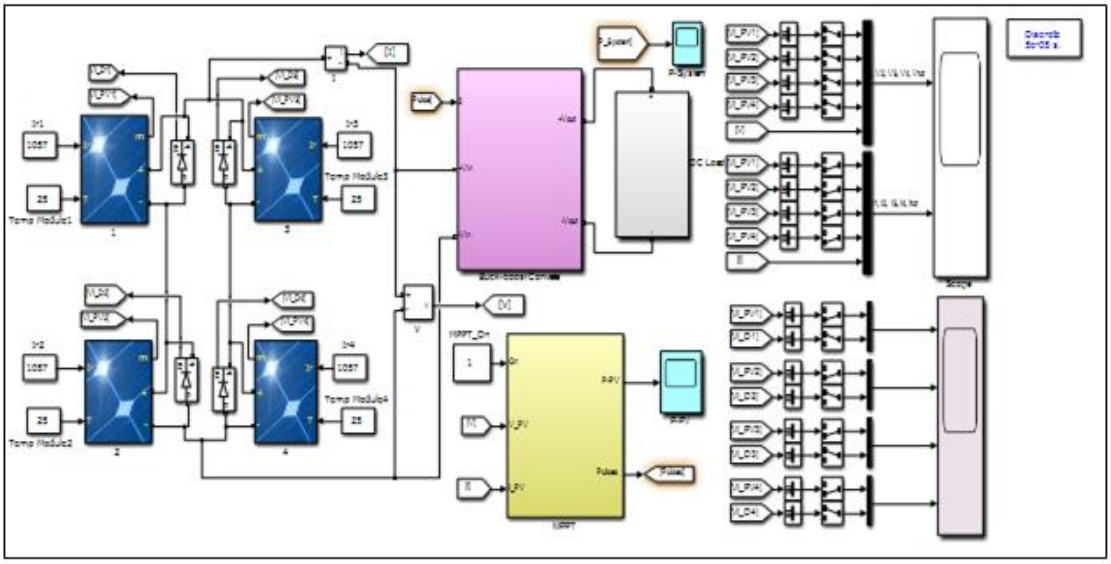

Fig 39: Simulink model of four modules where two are serially connected and two are linked in parallel; both temperature and shadow are constant in this system

The Seybold Report
ISSN 1533-9211
DOI: 10.5281/zenodo.14615527

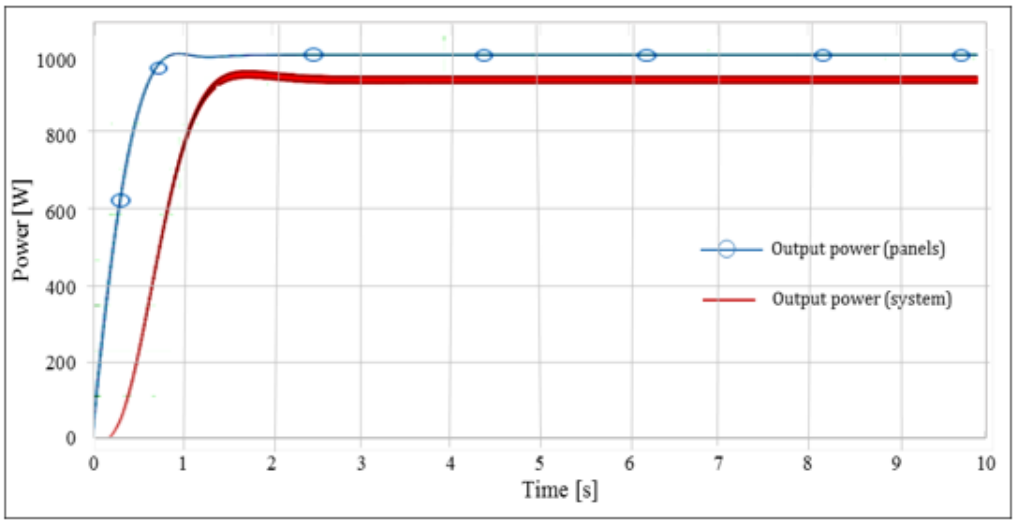

Fig 40: System's output power when two modules are serially connected and two are linked in parallel; both temperature and shadow are constant in this system

Figs. (41 and 42) show the Simulink model and output power of a system where the temperature is varied and shadow is constant; for this system, T = 10°C on one module. The system and modules' output are influenced inversely. Voltage increases at lower temperatures, and vice versa. The modules' output post-temperature effect = 930.8 W, whereas the system output = 875.3 W. A good efficiency of approximately 94% was achieved.

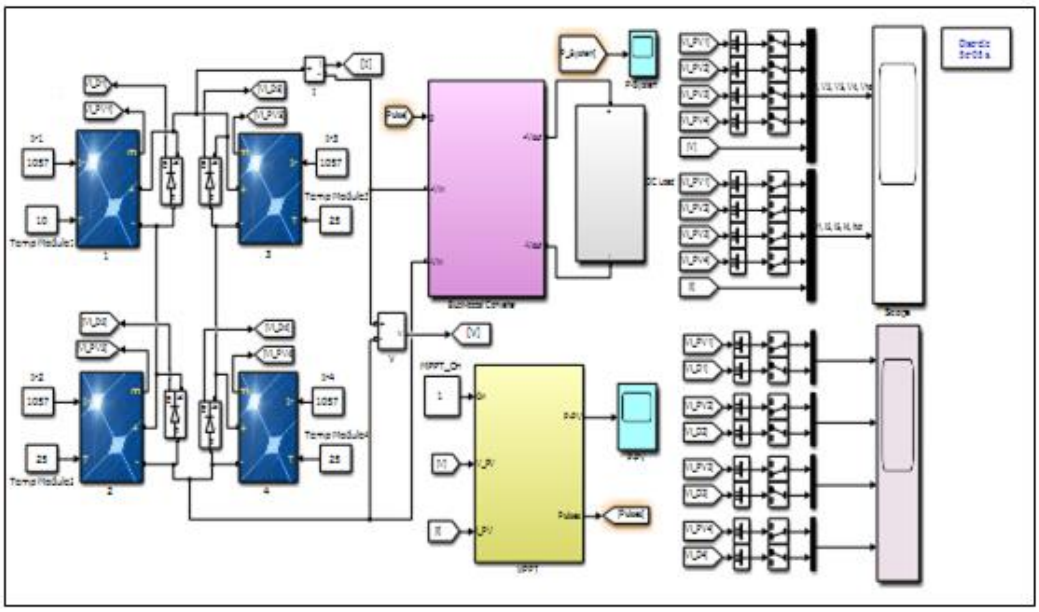

Fig 41: Simulink model of four modules where two are serially linked and two are in parallel; the shadow is fixed and T = 10°C at one module

The Seybold Report
ISSN 1533-9211
DOI: 10.5281/zenodo.14615527

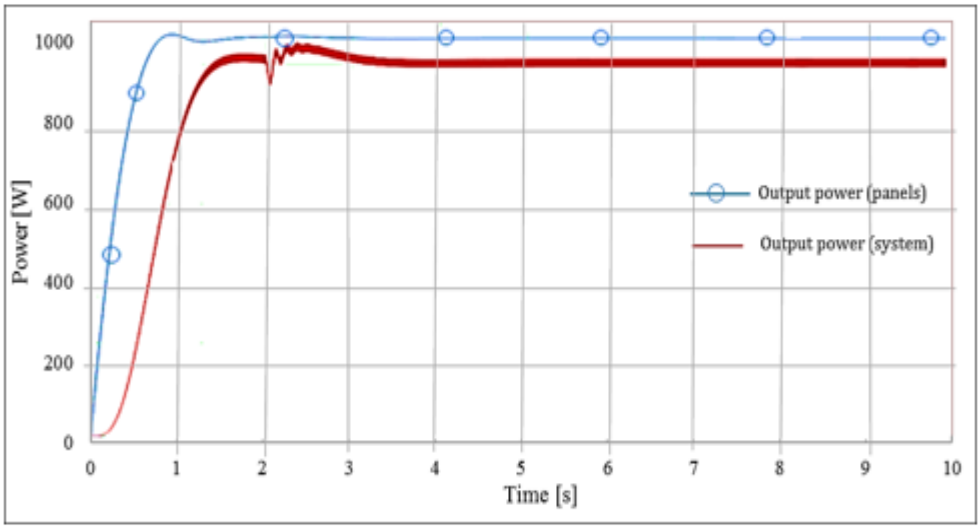

Fig 42: System's output power when two modules are serially connected and two are linked in parallel; the shadow is fixed and *T* = 10°C at one module

Figs. (43 and 44) depict the Simulink model and output power of a system where T = 50oC on one module and shadow is constant. The module and systems' output are inversely influenced. The modules' output post-temperature effect = 889.1 W, while the system's output = 841.2 W. Efficiency is good at approximately 94.6%.

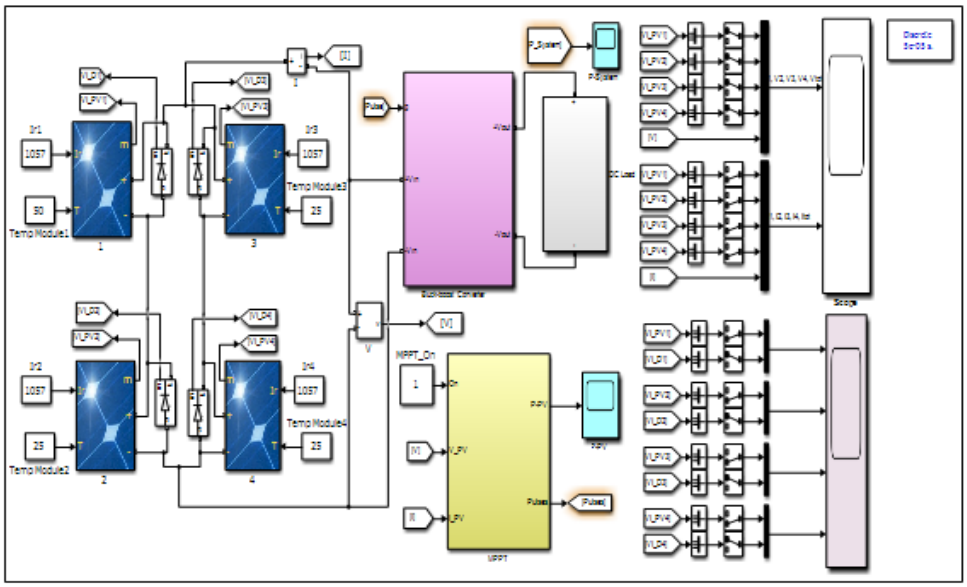

Fig 43: Simulink model of four modules where two are serially connected and two are linked in parallel; the shadow is fixed and *T* = 50°C at one module

The Seybold Report
ISSN 1533-9211
DOI: 10.5281/zenodo.14615527

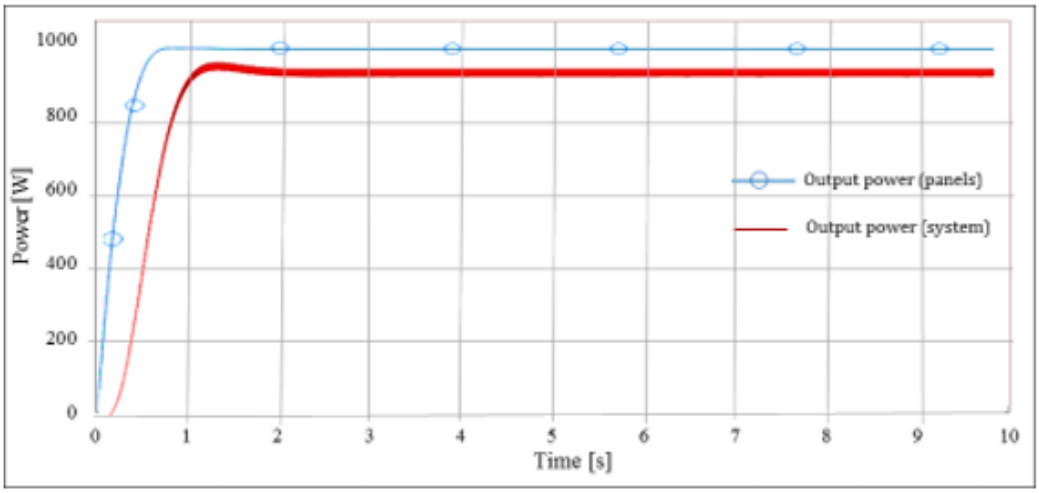

Fig 44: System's output power when two modules are serially connected and two are linked in parallel; the shadow is fixed and $T = 50^{o}C$ at one module

As shown in Table (2), two parameters can influence the connection of four modules in series and parallel- irradiance and temperature. The parallel connection of 4 modules produces better performance than their serial connection. Furthermore, as the irradiance declines, the output power of the modules drops dramatically. In contrast, when the temperature drops, the output power of the modules increases.

Table 2: Comparison of the output power for four modules connected in series at different temperatures and constant irradiance $G = 1057$ W/m^2

No.	Irradiances	T = 25° C	T = 10 ° C	T = 50 ° C
1	$G = 1057$ W/m^2	919.94 W	930.3 W	W

4. CONCLUSION

Several factors now encourage us to switch to renewable energy sources, including the rising expense of fossil fuels and growing awareness of climate change. Continuous technology and research will undoubtedly change solar energy into a more mature technology in the near future. The PV energy market has grown as a result of government targets for renewable energy generation and CO2 emission reductions, and the "International Energy Agency" has predicted total global reliance on solar energy by the year 2050.

This paper provides a complete presentation of solar PV systems, commencing with solar cells and their operating modalities, as well as solar cell efficiency. Considering the amazing developments in solar cell technology over the last few decades, the future of solar PV applications appears to be bright.

In the event of PV array partial shade, detecting global MPP is critical for maximizing PV system energy production. One of the biggest disadvantages is that partial shading reduces the maximum power output of the PV array. In partially shaded situations, where the P-V curve

The Seybold Report
ISSN 1533-9211
DOI: 10.5281/zenodo.14615527

has numerous local maximum values, a traditional MPPT algorithm typically follows less than the actual MPP, resulting in a significant loss in energy. The proposed PV system in this study responds and performs well in such situations. Even in situations where there is partial shading of the PV array, a PV system is expected to immediately operate at MPP. Therefore, this work described numerous methods for increasing solar power systems' efficiency, ranging from the structure of the solar cells to the module/array, and then to the DC-DC inversion. The P&O algorithm-based MPPT was also proposed as the ideal way for efficient conversion of solar energy. The majority of MPPT algorithms were analyzed in this work to determine the actual MPP and after analyzing the results, it is clear that the modified P&O performed best due to its simplicity and efficacy. Despite this, the P&O was chosen for additional examination in this study. The simulations were used to investigate P&O performance and dynamic MPPT efficiency.

The buck-boost converter simulation model was constructed in MATLAB/SIMULINK using the Perturb and Observe MPPT approach. The MPPT method utilized in this study improved both the dynamic and steady-state performance of the PV system. The simulation results indicated that the system was able to track the MPP despite the oscillations. When the external environment changes rapidly, the system could capture the MPP. However, the solar panel recorded just a small power loss to the buck-boost converter output, which might be attributed to switching losses as well as losses in the boost converter's capacitor and inductor, as shown by the relevant power curves. As a consequence, using the P&O MPPT approach increased the efficiency of the PV system. The study examines two factors that influence the performance of a solar PV array: irradiance and temperature. The results show that adjusting the irradiations only has a proportional effect on the I-V curve's current.

However, increasing the temperature has an inverse effect on the voltage in the I-V curve. The issue of performance efficiency following serial and parallel connection of the modules was also addressed. The results reveal that modules that are connected in parallel produced better outcomes than connecting the panels in series. Partial shading of one of the panels that are serially connected results in a similar effect on all the panels because the current is the same. This means that the panels' output power will be affected.

When partial shadowing strikes one panel of a set of panels connected in parallel, the effect does not extend to all of the panels because their currents differ. In the future, while considering how to integrate multiple solar arrays, there may be a need for one array to be partially shaded while the rest are under normal conditions. Furthermore, a set of serially-connected panels can be investigated in situations where one is shaded and the voltage exceeds zero.

The level of irradiation affects the output power, and high temperatures contribute to substantial power loss. This has affected the acceptability of solar energy as an excellent choice for electricity consumers. Therefore, as the main of this study is focused on improving solar PV's efficiency, however, to ensure that such efficiency is created, then the below-suggested recommendation must be taken into serious consideration.

The Seybold Report
ISSN 1533-9211
DOI: 10.5281/zenodo.14615527

These are as follows:

i. The researchers have recommended using solar PV panels with power generation greater than 230 W, nowadays PV modules with power generation up to 700 W;

ii. They have also recommended using ANN and Fuzzy Logic with MPPT for solar PV systems when some modules are partially shaded and results later could be compared; and

iii. The study recommended that the benefits or outcomes when solar PV systems must in the future be studied earlier prior to using it in the national electricity grid.

References

1) Aashoor, F., & Robinson, F. (2012). A variable step size perturb and observe algorithm for photovoltaic maximum power point tracking, 47th International Universities Power Engineering Conference (UPEC), pp. 1-6.

2) Alajmi, B.N., Ahmed, K.H., Finney, S.J., & Williams, B.W. (2010). Fuzzy-logic-control approach of a modified hill-climbing method for maximum power point in microgrid standalone photovoltaic system, IEEE Transactions on Power Electronics, 26, 1022-1030.

3) Alik, R., Jusoh, A., & Sutikno, T. (2017). A Study of Shading Effect on Photovoltaic Modules with Proposed P&O Checking Algorithm, International Journal of Electrical & Computer Engineering, 7(1), 29-40.

4) Alqarni, M., & Darwish, M.K. (2012). Maximum power point tracking for photovoltaic system: modified perturb and observe algorithm, 47th International Universities Power Engineering Conference (UPEC), 1-4.

5) Alrikabi, N. (2014). Renewable energy types, Journal of Clean Energy Technologies, 2, 61-64.

6) Avila, E., Pozo, N., Pozo, M., Salazar, G., & Domínguez, X. (2017). Improved particle swarm optimization based MPPT for PV systems under Partial Shading Conditions, IEEE Southern Power Electronics Conference (SPEC), pp. 1-6.

7) Behura, A.K., Kumar, A., Rajak, D.K., Pruncu, C.I., & Lamberti, L. (2021). Towards better performances for a novel rooftop solar PV system, Solar Energy, 216, 518-529.

8) Chiu, C.-S., & Ngo, S. (2023). Hybrid SFLA MPPT design for multi-module partial shading photovoltaic energy systems, International Journal of Electronics, 110, 199-220.

9) Elgendy, M.A., Zahawi, B., & Atkinson, D.J. (2012). Assessment of the incremental conductance maximum power point tracking algorithm, IEEE Transactions on Sustainable Energy, 4, 108-117.

10) Feng, X., & Ma, T. (2023). Solar photovoltaic system under partial shading and perspectives on maximum utilization of the shaded land, International Journal of Green Energy, 20, 378-389.

11) Fialho, L., Melicio, R. , Mendes, V., Figueiredo, J., & Collares-Pereira, M. (2014). Effect of shading on series solar modules: simulation and experimental results, Procedia Technology, 17, 295-302.

12) Hamidon, F., Aziz, P.A., & Yunus, N.M. (2012). Photovoltaic array modelling with P&O MPPT algorithm in MATLAB, International Conference on Statistics in Science, Business and Engineering (ICSSBE), pp. 1-5.

13) Ishaque, K., Salam, Z., & Lauss, G. (2014). The performance of perturb and observe and incremental conductance maximum power point tracking method under dynamic weather conditions, Applied Energy, 119, 228-236.

The Seybold Report
ISSN 1533-9211
DOI: 10.5281/zenodo.14615527

14) Ishaque, K., Salam, Z., Amjad, M., & Mekhilef, S. (2012). An improved particle swarm optimization (PSO)–based MPPT for PV with reduced steady-state oscillation, IEEE transactions on Power Electronics, 27, 3627-3638.

15) Johari, A., Hafshar, S.S., Ramli, M., & Hashim, H. (2011). Potential use of solar photovoltaic in Peninsular Malaysia, IEEE Conference on Clean Energy and Technology (CET), pp. 110-114.

16) Ngan, M.S., & Tan, C.W. (2011). A study of maximum power point tracking algorithms for stand-alone photovoltaic systems, IEEE applied power electronics colloquium (IAPEC), pp. 22-27.

17) Pva, A.N. (2011). Guide To Interpreting IV Curve Measurements of PV Arrays, Solmetric Application Note.

18) Ragb, O., & Bakr, H. (2023). A new technique for estimation of photovoltaic system and tracking power peaks of PV array under partial shading, Energy, 268, 126680.

19) Sharma, D., & Purohit, G. (2012). Advanced perturbation and observation (P&O) based maximum power point tracking (MPPT) of a solar photo-voltaic system, IEEE 5th India International Conference on Power Electronics (IICPE), pp. 1-5.

20) Singh, P., Palwalia, D., Gupta, A., & Kumar, P. (2015). Comparison of photovoltaic array maximum power point tracking techniques, International Advanced Research Journal in Science, Engineering and Technology, 2(1), 401-404.